Regulatory T cells control *Staphylococcus aureus* and disease severity of cutaneous leishmaniasis

Tej Pratap Singh[1,2] , Camila Farias Amorim[1] , Victoria M. Lovins[2] , Charles W. Bradley[1] , Lucas P. Carvalho[3,4] , Edgar M. Carvalho[3,4] , Elizabeth A. Grice[2] , and Phillip Scott[1]

Cutaneous leishmaniasis causes alterations in the skin microbiota, leading to pathologic immune responses and delayed healing. However, it is not known how these microbiota-driven immune responses are regulated. Here, we report that depletion of Foxp3+ regulatory T cells (Tregs) in *Staphylococcus aureus*–colonized mice resulted in less IL-17 and an IFN-γ–dependent skin inflammation with impaired *S. aureus* immunity. Similarly, reducing Tregs in *S. aureus*–colonized and *Leishmania braziliensis*–infected mice increased IFN-γ, *S. aureus*, and disease severity. Importantly, analysis of lesions from *L. braziliensis* patients revealed that low *FOXP3* gene expression is associated with high *IFNG* expression, *S. aureus* burden, and delayed lesion resolution compared to patients with high *FOXP3* expression. Thus, we found a critical role for Tregs in regulating the balance between IL-17 and IFN-γ in the skin, which influences both bacterial burden and disease. These results have clinical ramifications for cutaneous leishmaniasis and other skin diseases associated with a dysregulated microbiome when Tregs are limited or dysfunctional.

Introduction

Cutaneous leishmaniasis is caused by infection with the protozoan parasite *Leishmania,* and the resulting pathology ranges from mild cutaneous lesions to chronic non-healing and metastatic disease. Unfortunately, there is no vaccine for this disease, and anti-leishmania drugs are often toxic and marginally effective (Kaye and Scott, 2011; Scott and Novais, 2016; Unger et al., 2009). While infection-induced immune responses are critical for parasite control, they can also result in immunopathology, which largely dictates the clinical presentation. For example, while parasite control depends upon killing by IFN-γ–activated macrophages, an exaggerated immune response leads to more severe disease (Ehrlich et al., 2014; Gonzalez-Lombana et al., 2013; Kaye and Scott, 2011; Pandiyan et al., 2019; Scott and Novais, 2016). Understanding the factors driving this increased disease can provide targets for better therapy.

We and others found that increased IL-1β production promotes a severe inflammatory response in cutaneous leishmaniasis without playing a role in parasite control (Charmoy et al., 2016; Gonzalez-Lombana et al., 2013; Novais et al., 2017; Santos et al., 2018). One factor driving increased IL-1 in leishmaniasis is bacteria associated with the skin microbiome (Gimblet et al., 2017; Naik et al., 2012; Singh et al., 2021). Consistent with this,

we previously found that cutaneous leishmaniasis is associated with a dysregulated skin microbiome and, in many patients, increased *Staphylococcus aureus* (Amorim et al., 2023, *Preprint*; Gimblet et al., 2017). In mice, we found that a dysregulated skin microbiome promotes increased IL-1β levels and lesion severity (Gimblet et al., 2017), and *Leishmania braziliensis* patients with a high level of *S. aureus* in their lesions were delayed in healing (Amorim et al., 2023, *Preprint*). While *S. aureus* can silently colonize healthy individuals (Clegg et al., 2021), it also causes most skin and soft tissue infections and mediates pathology in many inflammatory dermatological diseases (Alekseyenko et al., 2013; Fyhrquist et al., 2019; Kobayashi et al., 2015; Terui et al., 2022). *S. aureus*, as well as other microbes, stimulates the IL-1 pathway and type-17 responses that are essential for bacteria control but also promotes increased inflammation (Brown et al., 2014; Cho et al., 2010; Liu et al., 2017; Miller and Cho, 2011; Nakagawa et al., 2017). These results implicate *S. aureus* colonization of leishmanial lesions as an important factor promoting increased disease. Given the potential for increased disease driven by excessive inflammation, we hypothesized that regulatory T cells (Tregs) would play a critical role in maintaining the balance between inflammation and control of bacteria by

[1]Department of Pathobiology, School of Veterinary Medicine, University of Pennsylvania, Philadelphia, PA, USA; [2]Department of Dermatology, Perelman School of Medicine, University of Pennsylvania, Philadelphia, PA, USA; [3]Servico de Imunologia, Complexo Hospitalar Universitario Professor Edgard Santos, Universidade Federal da Bahia, Salvador, Brazil; [4]Laboratorio de Pesquisas Clinicas do Instituto de Pesquisas Goncalo Moniz, Fiocruz, Salvador, Brazil.

Correspondence to Phillip Scott: pscott@vet.upenn.edu.

limiting the IL-17 response. Tregs are critical for preventing chronic dermal inflammation and, depending on the context, can block a diverse set of immune responses (Boothby et al., 2020; Whibley et al., 2019). Tregs are primed by bacteria in neonates to promote tolerance to skin microbiota later in life, although such tolerance is not initiated with *S. aureus* (Leech et al., 2019; Scharschmidt et al., 2015). Most Tregs in the skin express GATA3 and regulate Th2 responses (Boothby et al., 2021; Kalekar et al., 2019; Wohlfert et al., 2011), although, in other contexts, they may also regulate IL-17 and IFN-γ responses (Mathur et al., 2019; Moreau et al., 2021; Nosbaum et al., 2016). In leishmaniasis, IL-10 limits the complete clearance of the parasites but may also limit disease severity (Belkaid et al., 2002; Ehrlich et al., 2014; Gonzalez-Lombana et al., 2013). While IL-10 can be produced by Tregs, in leishmaniasis, other cells have been shown to be the primary source of IL-10 (Anderson et al., 2007; Bunn et al., 2018), leaving open the question of Treg's role in cutaneous leishmaniasis when a *S. aureus* dysbiosis has developed.

In this study, we used a clinical isolate of *S. aureus* from a patient infected with *L. braziliensis* to investigate how the host immune response is impacted in mice colonized with *S. aureus*. While skin colonization with *S. aureus* induced a dominant IL-17 response that exacerbated disease severity in *L. braziliensis*–infected mice, it also promoted the accumulation of Tregs. We unexpectedly found that Tregs facilitate IL-17–dependent *S. aureus* immunity. Specifically, the depletion of Tregs in *S. aureus*–colonized mice led to a decreased IL-17 response and increased IFN-γ, leading to epidermal damage and an increased *S. aureus* burden. In contrast to the dominant role of GATA3^{+} Tregs in tissue repair and Th2 responses within the skin (Boothby et al., 2020; Kalekar et al., 2019; Wohlfert et al., 2011), we found that a subset of RORγt-expressing Foxp3^{+} Tregs was important in regulating the pathogenic type 1 response in the context of *S. aureus*. Not only were Tregs contributing to the maintenance of the IL-17 response and control of the bacterial burden in mice colonized with *S. aureus*, partial reduction of Tregs in *S. aureus*–colonized and *L. braziliensis*–infected mice increased IFN-γ responses, disease severity, and *S. aureus* burden. Importantly, our findings appear clinically significant as a transcriptional analysis of biopsies of lesions from *L. braziliensis* patients revealed that low levels of *FOXP3* transcripts were associated with increased expression of *IFNG* and a delay in healing, suggesting that variability in the number of Tregs in patient's lesions influence disease severity. These results uncover a previously unappreciated role for Tregs in regulating opportunistic *S. aureus* infection by moderating IFN-γ–mediated pathology.

Results

S. aureus–induced immune responses exacerbate disease severity in cutaneous leishmaniasis

We found that *Staphylococcus* species often dominate the lesional microbiota of cutaneous leishmanial infections in both mice and patients and can be associated with more severe disease and delays in lesion resolution (Amorim et al., 2023, *Preprint*;

Gimblet et al., 2017). *S. aureus* was the most frequent species cultured from human *L. braziliensis* lesions and a clinical isolate was selected for subsequent experiments to delineate how *Staphylococcus* influences disease outcome (Amorim et al., 2023, *Preprint*). We topically colonized mice on four consecutive days with *S. aureus* to assess how the bacteria influences skin immune responses (Fig. 1 A) and found that *S. aureus* could be cultured from the skin for at least 30 d following colonization (Fig. S1 A). We quantified *Ifng*, *Il13*, and *Il17a* transcripts and found significantly higher gene expression of *Il17a* and *Ifng* but not *Il13* in *S. aureus*–colonized mice compared with control mice (Fig. 1 B). Next, we performed flow cytometry to identify the cell types producing IL-17A and IFN-γ (Fig. S1 B). The dominant producers of IL-17A were γδ^{low} T cells, although all T cell subsets and innate lymphoid cells (ILCs) exhibited increased IL-17A levels (Fig. 1, C–G and I; and Fig. S1 C). IFN-γ was also increased in *S. aureus*–colonized mice and was mainly found in T cells (Fig. 1, E, F, H, and I; and Fig. S1 C). In addition, the total number of γδ^{low} T cells, CD4 T cells, and ILCs were markedly increased in the skin after *S. aureus* colonization compared with control mice (Fig. 1 J). We analyzed arrays of chemokines and cytokines to identify genes expressed in the ear skin of *S. aureus*–colonized mice. The transcripts associated with an IL-17 signature, including *Il1b*, *Il6*, *Il23a*, *Ccl20*, and *Cxcl1*, were induced in *S. aureus*–colonized skin compared with control skin (Fig. S1, D and E). Despite these changes, *S. aureus* colonization without skin injury was associated with minimum skin inflammation, suggesting some regulation of the response to *S. aureus* (Fig. S1 F). Taken together, these data indicate that despite minimal skin thickening, colonization with *S. aureus* in the skin induces a T cell response dominated by IL-17.

To determine whether *S. aureus*–colonized mice would develop more severe disease in cutaneous leishmaniasis, we colonized the mice with *S. aureus* and infected them with *L. braziliensis* (Fig. 2 A). *S. aureus* colonization significantly augmented lesion size and skin pathology following infection with *L. braziliensis* (Fig. 2, B and C), consistent with previous findings that *Staphylococcus* colonization exacerbates disease in cutaneous leishmaniasis (Gimblet et al., 2017; Naik et al., 2012). The augmented disease was not associated with increased parasites but was characterized by increased epidermal thickening and infiltration of inflammatory cells in the epidermis and dermis (Fig. 2, D and E). The absolute numbers of γδ^{low} T cells and IL-17A^{+}γδ^{low} T cells were significantly increased in mice with *S. aureus* compared with control groups (Fig. 2 F), with no significant changes in IFN-γ–producing CD4^{+} T cells (Fig. 2 G). We found a significant increase in neutrophils in *S. aureus*–colonized mice (Fig. 2 H), which, while required for immunity against *S. aureus* (Cho et al., 2010; Miller and Cho, 2011), enhances disease in cutaneous leishmaniasis (Boaventura et al., 2010; Goncalves-de-Albuquerque et al., 2017; Pedraza-Zamora et al., 2017). We found that the increase in neutrophils was dependent upon IL-1β (Amorim et al., 2023, *Preprint*). Similarly, blocking IL-17 reduced the inflammation in *L. braziliensis*–infected and *S. aureus*–colonized mice and increased the *S. aureus* burden (Fig. S1 G). These results are consistent with previous studies showing that IL-17 promotes increased disease in cutaneous
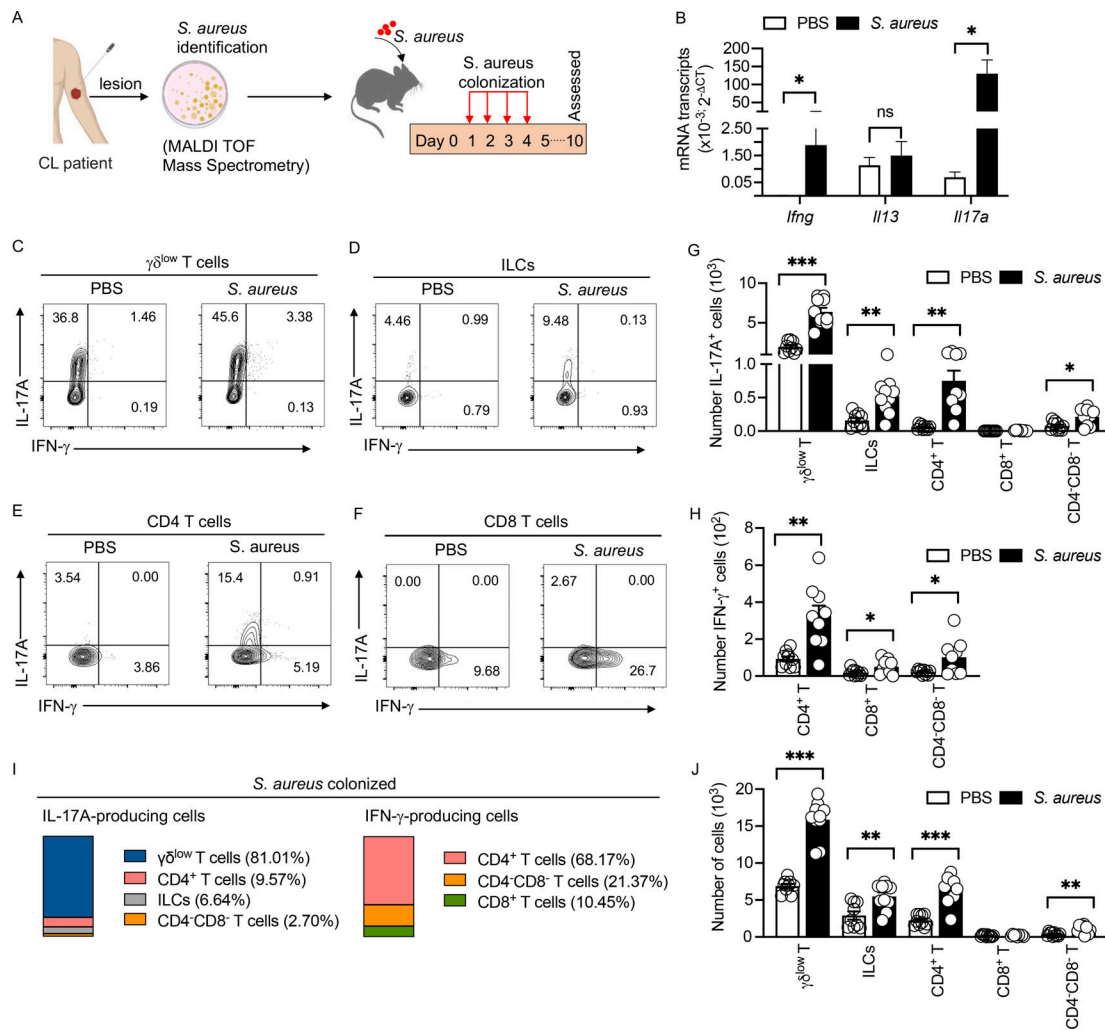
Figure 1. Immune signature in uninjured skin after topical _S. aureus_ colonization. (A) Clinical _S. aureus_ isolate colonization protocol. C57BL/6 mice were colonized with a clinical _S. aureus_ isolate from the skin lesions of a _L. braziliensis_–infected patient on day 1–4 and euthanized on day 10 for ear skin collection and analysis. MALDI TOF, Matrix-assisted laser desorption/ionization-time of flight. **(B)** mRNA analysis by qRT-PCR for _Ifng_, _Il13_, and _Il17a_ transcripts in _S. aureus_–colonized and PBS control mice on day 10. Mean ± SEM from two experiments with five mice per group. **(C–F)** Flow cytometry analysis of IL-17A and IFN-γ production from γδ^{low} T cells, ILCs, CD4^{+} T cells, and CD8^{+} T cells in uncolonized (PBS, control) and _S. aureus_–colonized mice on day 10. Representative of two experiments with 9–10 mice per group. Numbers in contour plots indicate the percent of cells within the gates. **(G)** Absolute numbers of IL-17A–producing γδ^{low} T, ILCs, CD4^{+} T, CD8^{+} T, and CD4^{−}CD8^{−} T cells in uncolonized (PBS, control) and _S. aureus_–colonized mice on day 10. Mean ± SEM from two experiments with 9–10 per mice group. **(H)** Absolute numbers of IFN-γ–producing CD4^{+} T, CD8^{+} T, and CD4^{−}CD8^{−} T cells in uncolonized (PBS, control) and _S. aureus_–colonized mice on day 10. Mean ± SEM from two experiments with 9–10 mice per group. **(I)** Contribution of IL-17A and IFN-γ from T cells and ILCs within the ear skin of _S. aureus_–colonized mice at day 10. Absolute numbers were used to create the chart. Two experiments with 9–10 mice per group. **(J)** Absolute numbers of γδ^{low} T cells, ILCs, CD4^{+} T, CD8^{+} T, and CD4^{−}CD8^{−} T cells in uncolonized (PBS, control) and _S. aureus_–colonized mice on day 10 by flow cytometry. Mean ± SEM from two experiments with 9–10 mice per group. *P < 0.05, **P < 0.01, and ***P < 0.001. "ns" denotes not significant. Significant P values by two-tailed unpaired Student's _t_ test with Welch's correction are indicated in the figure.

leishmaniasis (Gonzalez-Lombana et al., 2013; Lopez Kostka et al., 2009; Singh et al., 2021). To determine if these results were unique to _S. aureus_ and _L. braziliensis_, we also tested if _S. aureus_ promoted increased IL-17 and disease using a TLR7-ligand–induced dermatitis model (Fig. 2 I), which promotes skin inflammation through IL-23–dependent IL-17 secretion (van der Fits et al., 2009). We similarly found enhanced skin inflammation in _S. aureus_–colonized mice and increased γδ^{low} T cells and IL-17 production by γδ^{low} T cells (Fig. 2, J–L). Together, these studies extend our previous work, demonstrating that _S. aureus_ promotes increased disease.

Foxp3 Tregs limit cutaneous inflammation and _S. aureus_ abundance

A large percentage of the CD4^{+} T cells present in the skin of mice and humans are Foxp3^{+}, where they inhibit autoimmunity and promote tissue maintenance (Boothby et al., 2020; Gouirand et al., 2022; Whibley et al., 2019). Since _S. aureus_ colonization alone induced minimal inflammation, we hypothesized that Tregs might be critical to limit inflammation mediated by IL-17. Consistent with this, we observed an accumulation of Tregs in the skin of _S. aureus_–colonized mice compared with control mice (Fig. 3 A), and the number of Ki67^{+} Tregs were also
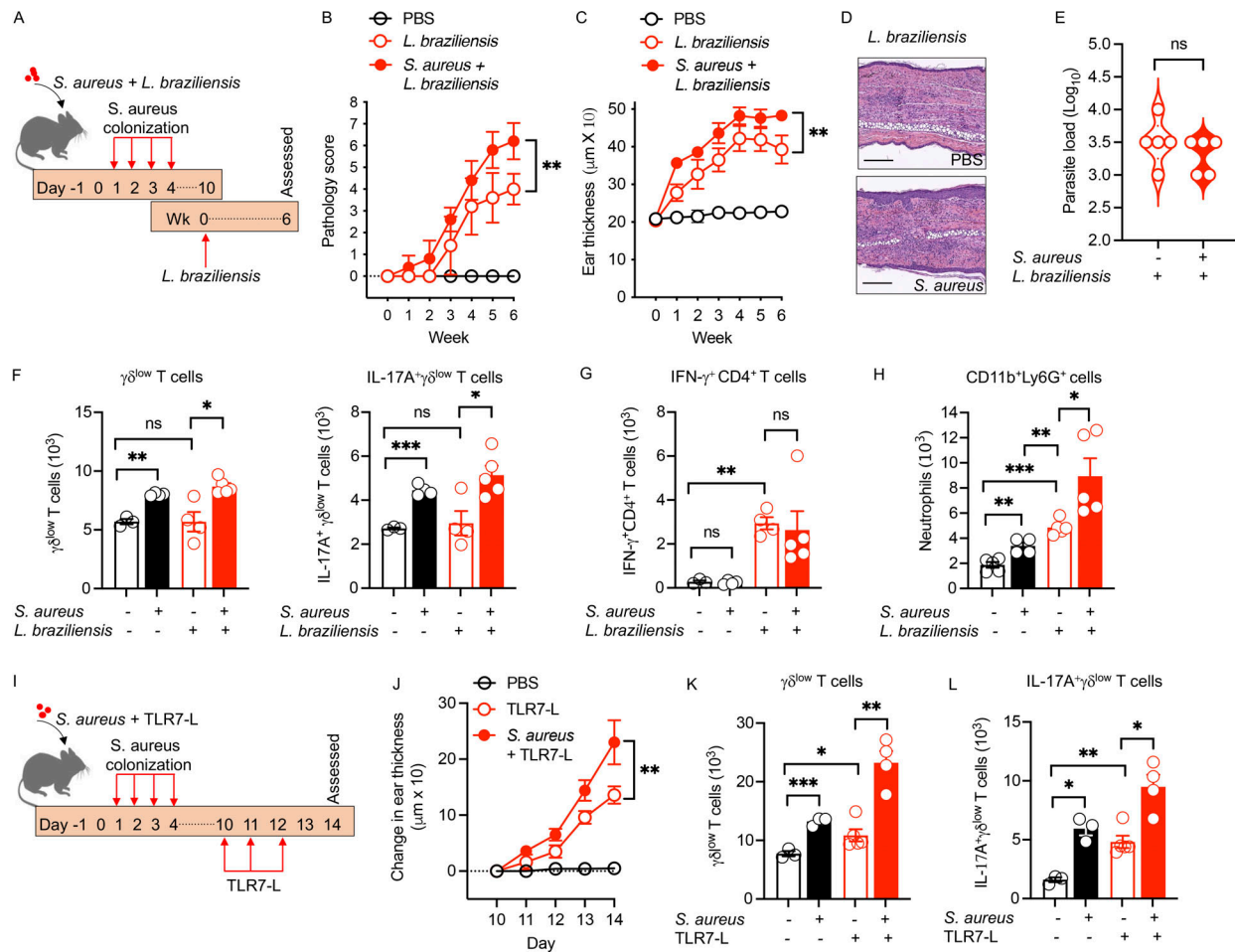
Figure 2. S. aureus augments pathology of cutaneous leishmaniasis and dermatitis. (A) Clinical *S. aureus* colonization and *L. braziliensis* infection protocol. C57BL/6 mice were colonized with *S. aureus* on days 1–4 and then on day 10 (week 0) mice were infected with *L. braziliensis*. Mice were euthanized at week 6 for tissue collection and analysis. **(B and C)** Pathology score (B) or ear thickness (C) of *S. aureus*–colonized or PBS control mice infected with *L. braziliensis* was assessed. Mean ± SD representative of two experiments with five mice per group. **(D)** H&E-stained ear sections of *S. aureus*–colonized or PBS control mice infected with *L. braziliensis* at week 6. Scale bar = 200 µm. **(E)** Parasite load in *S. aureus*–colonized or PBS control mice infected with *L. braziliensis* at week 6. Representative of two experiments with five mice per group. **(F)** Absolute numbers of γδ^{low} T cells and IL-17A$^+$γδ^{low} T cells of *S. aureus*–colonized or PBS control mice infected or non-infected with *L. braziliensis*. Mean ± SEM representative of two experiments with three to five mice per group. **(G)** Absolute numbers of IFN-γ$^+$CD4$^+$ T cells of *S. aureus*–colonized or PBS control mice infected or non-infected with *L. braziliensis*. Mean ± SEM representative of two experiments with three to five mice per group. **(H)** Absolute numbers of CD11b$^+$Ly6G$^+$ cells of *S. aureus*–colonized or PBS control mice infected or non-infected with *L. braziliensis*. Mean ± SEM representative of two experiments with four to five mice per group. **(I)** *S. aureus* colonization and TLR7-L (imiquimod) treatment protocol. 6-wk-old C57BL/6 mice were colonized with *S. aureus* at days 1–4 and then treated with TLR7-L every day for 3 d (days 10, 11, and 12). Mice were euthanized on day 14 for tissue collection and analysis. **(J)** Skin thickness measurement of *S. aureus*–colonized or PBS control mice treated with TLR7-L. Mean ± SD representative of two experiments with five mice per group. **(K and L)** Absolute numbers of γδ^{low} T cells and IL-17A$^+$γδ^{low} T cells of *S. aureus*–colonized or PBS control mice treated or non-treated with TLR7-L. Mean ± SEM representative of two experiments with three to five mice per group. *P < 0.05, **P < 0.01, and ***P < 0.001. "ns" denotes not significant. Significant P values by two-tailed unpaired Student's *t* test with Welch's correction are indicated in the figure.

increased in *S. aureus*–colonized mice (Fig. 3, B and C). Phenotypically, Foxp3$^+$ Tregs expressed ICOS, CTLA4, and CD25 but not ST2 (Fig. 3 D). These data suggest that *S. aureus* colonization increases the peripheral accumulation of proliferative Tregs in the skin. To determine if Tregs impact immune responses in *S. aureus*–colonized mice, we transiently depleted Tregs using Foxp3-DTR transgenic mice, which express the diphtheria toxin receptor (DTR) under the control of Foxp3 promoter (Kim et al., 2007). Foxp3 is expressed by CD4 T cells (Fig. S2 A), and treatment with diphtheria toxin (DT) in Foxp3-DTR mice allows for inducible depletion of Foxp3$^+$ Tregs. While the

long-term absence of Tregs leads to autoimmunity, a transient lack of Tregs does not induce skin inflammation (Ali et al., 2017; Hartwig et al., 2018). We treated the mice with DT (Fig. 3 E) and found that *S. aureus* burdens were substantially increased in these mice (Fig. 3 F), both in the epidermis and dermis (Fig. 3 G), and led to the dissemination of *S. aureus* to the skin-draining lymph node (Fig. 3 H). In addition, depletion of Tregs resulted in compromised skin barrier integrity as measured by transepidermal water loss (Fig. 3 I) and an increase in skin thickness, epidermal damage, and inflammatory cell infiltration into the skin as compared with Treg-sufficient mice
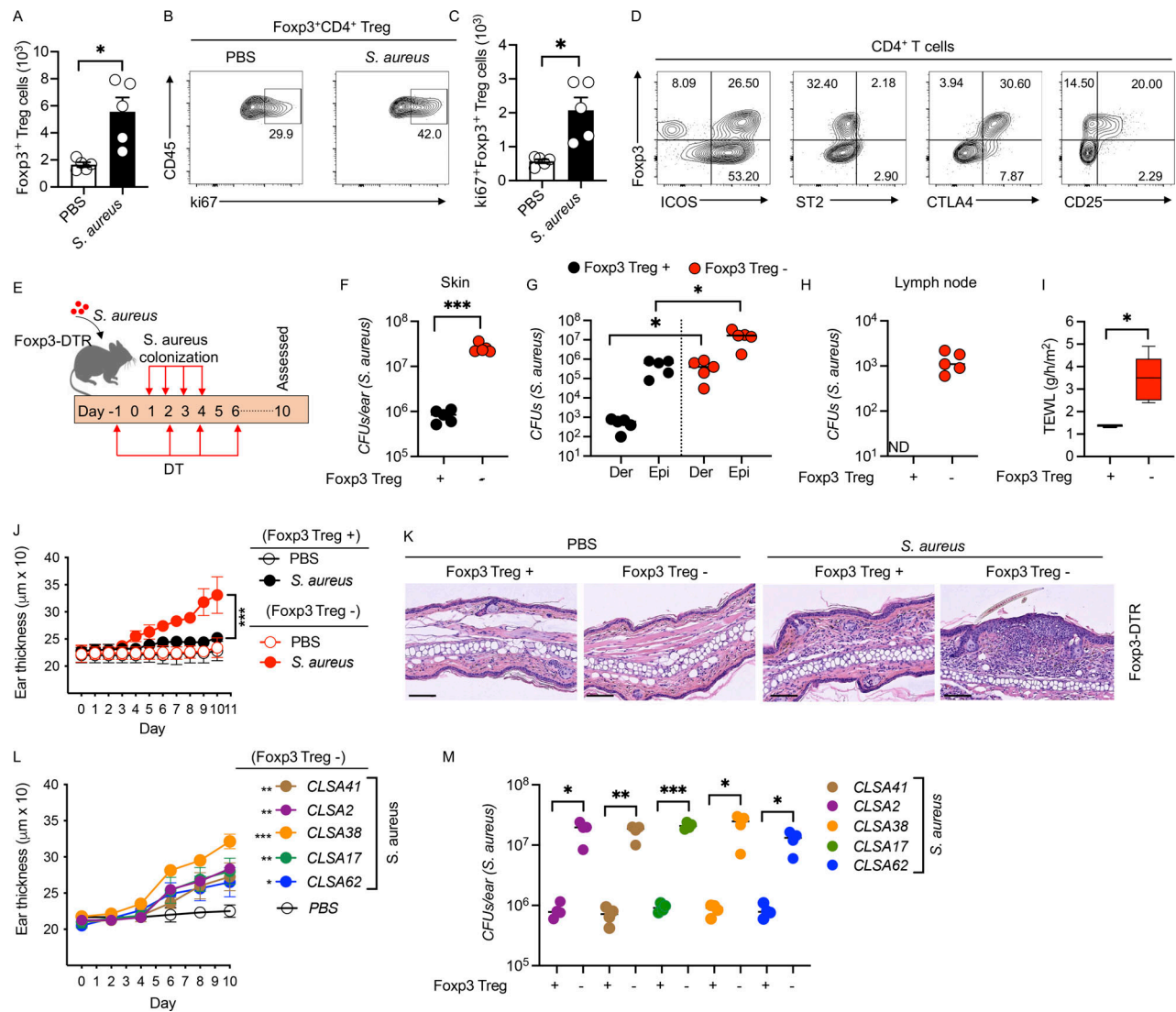
Figure 3. **Depletion of Foxp3⁺ Tregs facilitates *S. aureus* growth and spontaneous inflammation.** C57BL/6 mice were colonized with a clinical *S. aureus* as in Fig. 1 A and euthanized on day 10 for ear skin collection and analysis. **(A)** Absolute numbers of Foxp3⁺ Tregs in the skin of PBS and *S. aureus*–colonized mice on day 10. Mean ± SEM representative of two experiments with five mice per group. **(B and C)** Percent (B) and number (C) of Ki67⁺Foxp3⁺ Tregs in the skin of PBS and *S. aureus*–colonized mice at day 10. Mean ± SEM representative of two experiments with five mice per group. Numbers in contour plots indicate the percent of cells within the gates. **(D)** Analysis of ICOS, ST2, CTLA4, and CD25 expression on Foxp3⁺ Tregs. Representative of two experiments with six mice per group. Numbers in contour plots indicate the percent of cells within the gates. **(E)** *S. aureus* colonization protocol in Foxp3⁺ Treg-depleted or non-depleted Foxp3-DTR mice. Mice were colonized on days 1–4 and euthanized on day 10 for ear skin collection and analysis. Mice received DT on days −1, 2, 4, and 6. **(F)** CFUs of *S. aureus* at day 10 from the ear skin of *S. aureus*–colonized Foxp3-DTR mice depleted (Foxp3⁺ Treg⁻) or not (Foxp3⁺ Treg⁺) of Foxp3⁺ Tregs by DT treatment. Representative of two experiments with five mice per group. **(G)** CFUs of *S. aureus* at day 10 from the dermis (Der) and epidermis (Epi) ear skin of *S. aureus*–colonized Foxp3-DTR mice depleted or not of Tregs by DT treatment. Representative of two experiments with five mice per group. **(H)** CFUs of *S. aureus* at day 10 from the skin-draining lymph node of *S. aureus*–colonized Foxp3-DTR mice depleted or not of Tregs by DT treatment. Representative of two experiments with five mice per group. **(I)** Transepidermal water loss (TEWL) in *S. aureus*–colonized Foxp3-DTR mice depleted or not of Tregs by DT treatment. Representative of two experiments with four to five mice per group. **(J)** Ear thickness measurement in Foxp3-DTR mice depleted or not of Tregs by DT treatment, with and without *S. aureus* colonization. Mean ± SD representative of two experiments with five mice per group. **(K)** H&E-stained sections of Foxp3⁺ Treg cells non-depleted (Foxp3⁺ Treg⁺) and depleted (Foxp3⁺ Treg⁻) Foxp3-DTR mice colonized with *S. aureus* or non-colonized PBS control mice. Scale bar = 200 μm. **(L)** Ear thickness measurement in Foxp3-DTR mice depleted of Tregs and colonized with different clinical *S. aureus* isolates from *L. braziliensis* patients. Mean ± SD representative of two experiments with five mice per group. **(M)** CFUs of different clinical *S. aureus* isolates on day 10 from the ear skin of *S. aureus*–colonized, Treg non-depleted (Foxp3⁺ Treg⁺) and depleted (Foxp3⁺ Treg⁻) in Foxp3-DTR mice. Representative of two experiments with four mice per group. *P < 0.05, **P < 0.01, and ***P < 0.001. Significant P values by two-tailed unpaired Student's *t* test with Welch's correction, except L, which is one-way ANOVA with Dunnett's multiple correction, are indicated in the figure.

(Fig. 3, J and K). These results suggest that Foxp3+ Tregs not only limit tissue damage but also may play a critical role in limiting colonization by opportunistic bacteria. To investigate if the inflammatory responses we observed in the absence of Tregs were limited to one specific isolate of *S. aureus*, we colonized Treg-depleted mice with additional *S. aureus* isolates from *L. braziliensis* patients. While there were slight differences in the degree of inflammation as assessed by ear thickness, all the strains promoted increased skin thickening and were associated with increased *S. aureus* levels in Treg-depleted mice (Fig. 3, L and M). These results suggest that Tregs limit opportunistic bacterial colonization and tissue damage.

Foxp3+ Tregs control a pathogenic type 1 immune response

To understand how Tregs were influencing *S. aureus* levels, we performed flow cytometry on cells from the skin of Treg-depleted and Treg-sufficient mice after *S. aureus* colonization. In *S. aureus*–colonized, Treg-depleted mice, we found a higher accumulation of CD4+ and CD8+ T cells compared with Treg-sufficient mice but no differences in the number of γδ^{low} T cells (Fig. 4 A). *S. aureus*–colonized, Treg-depleted mice also had a higher percentage of CD4+ and CD8+ T cells compared with controls (Fig. 4 B). To investigate if the absence of Tregs impacted the IL-17 and IFN-γ responses that we observed in *S. aureus*–colonized mice, we analyzed cytokine production from T cells by flow cytometry. Since we previously found that blocking IL-10 led to an IL-17–dependent increase in disease in leishmaniasis, we expected a similar response when we depleted Tregs (Gonzalez-Lombana et al., 2013) as Foxp3+ Tregs in the skin can produce IL-10 (Fig. S2 B). Instead, we found that Treg depletion decreased IL-17 from γδ^{low} and CD4 T cells (Fig. 4, C–F). Expression of other pathogenic cytokines, including GM-CSF, IL-22, and TNFα, were not significantly increased (Fig. S2 C). In contrast to IL-17, the number and percentage of IFN-γ–producing cells were significantly increased in CD4 and CD8 T cells, with a more moderate increase in IL-5 and IL-13 expression, compared with controls (Fig. 4, C–H; and Fig. S2 D). Consistent with the increased IFN-γ, we found that a high percentage of CD4 and CD8 T cells expressed T-bet (Fig. 4 I). We also found that Treg depletion led to an increase in monocytes (Fig. 4 J). Since IFN-γ and IL-17 are known to crossregulate each other (Hu and Ivashkiv, 2009), it was possible that the increased levels of IFN-γ were responsible for the diminished IL-17 response. If this was the case, depletion of IFN-γ in *S. aureus*–colonized mice without Treg depletion might increase the IL-17 response and lead to better control of *S. aureus*. To test this, we colonized IFN-γ–deficient mice (IFN-γ$^{-/-}$) with *S. aureus* and assessed IL-17 responses and found that IFN-γ$^{-/-}$ mice produced higher levels of IL-17 with increased numbers of γδ^{low} T cells and IL-17–producing γδ^{low} T cells in the skin, but not an increase in IL-17–producing CD4 T cells or ILCs (Fig. 4, K–M; and Fig. S2 E) without impacting the number of Foxp3+ Tregs (Fig. S2 F). The absence of both IFN-γ and Tregs led to greater IL-17 induction, suggesting that Tregs also play a role in regulating IL-17 in *S. aureus*–colonized mice (Fig. S2 G). We also observed a significant decrease in *S. aureus* in the IFN-γ$^{-/-}$ mice (Fig. 4 N), which we believe is due to the increased production of IL-17. We confirmed

our results in knockout mice by treating *S. aureus*–colonized mice with anti–IL-17 or anti–IFN-γ antibodies. Like IFN-γ$^{-/-}$ mice, we observed decreased *S. aureus* burdens in anti–IFN-γ treated mice compared with control mice, while mice treated with anti–IL-17 exhibited a higher *S. aureus* burden (Fig. 4 O). These data highlight a crucial role for Tregs in blocking a pathogenic type 1 immune response, thereby facilitating a strong IL-17 response that can control *S. aureus*.

IFN-γ mediates increased inflammation, epidermal damage, and *S. aureus* burden

We hypothesized that the increased production of IFN-γ not only limited IL-17 responses but was mediating the increased severity of disease in *S. aureus*–colonized mice when Tregs were depleted. To test this, we neutralized IFN-γ in *S. aureus*–colonized mice depleted of Tregs. Blocking IFN-γ significantly reduced skin thickening and histological alterations we observed in control mice (Fig. 5, A and B). As anticipated, the number of IL-17–producing γδ^{low} T cells was restored in *S. aureus*–colonized and Treg-depleted mice after IFN-γ neutralization (Fig. 5 C). Additionally, blocking IFN-γ significantly reduced the number of CD4 T cells, CD8 T cells, and monocytes in *S. aureus*–colonized and Treg-depleted mice (Fig. 5 C). In addition, the transcripts associated with an IL-17 signature *Il6*, *Ccl20*, *S100a8*, and *Cxcl1* were increased after IFN-γ neutralization in Treg-depleted mice (Fig. 5 D). Further demonstrating the role of IL-17 in control of *S. aureus*, neutralization of IFN-γ in the absence of Tregs reduced the bacterial burden and migration of bacteria to the lymph node (Fig. 5 E). Since IFN-γ induces keratinocyte (KC) apoptosis and can enhance cell-mediated cytotoxicity (Rebane et al., 2012; Shao et al., 2019; Viard-Leveugle et al., 2013), we tested if the increased production of IFN-γ when Tregs are depleted in *S. aureus*–colonized mice might be promoting increased cell death. We observed significantly more dead epidermal cells in Treg-depleted mice compared with Treg-sufficient mice colonized with *S. aureus* (Fig. 5, F and G), and blocking IFN-γ increased the survival of the epidermal cells (Fig. 5, F and G). Furthermore, in vitro–treated primary human KCs with IFN-γ led to cell death in *S. aureus*–exposed KCs compared with control (Fig. 5 H). These data suggest that excess IFN-γ is directly involved in promoting epidermal destruction leading to *S. aureus* invasion/infection.

Foxp3+ Treg cells expressing RORγt control type 1 immune responses

Microbiota-dependent Foxp3+ Tregs are heterogeneous and comprise subsets uniquely poised to control specific immune responses (Pandiyan et al., 2019; Whibley et al., 2019). In normal skin, most Tregs express the transcription factor GATA3 and are involved in controlling skin fibrosis, wound healing responses, and barrier repair (Kalekar et al., 2019; Whibley et al., 2019; Wohlfert et al., 2011). To investigate the impact of *S. aureus* colonization on the phenotype of Tregs in the skin, we performed flow cytometry to quantify subsets of Tregs in *S. aureus*–colonized mice. As expected, most Tregs in the skin of control mice expressed GATA3. However, the number of Tregs expressing RORγt significantly increased in *S. aureus*–colonized
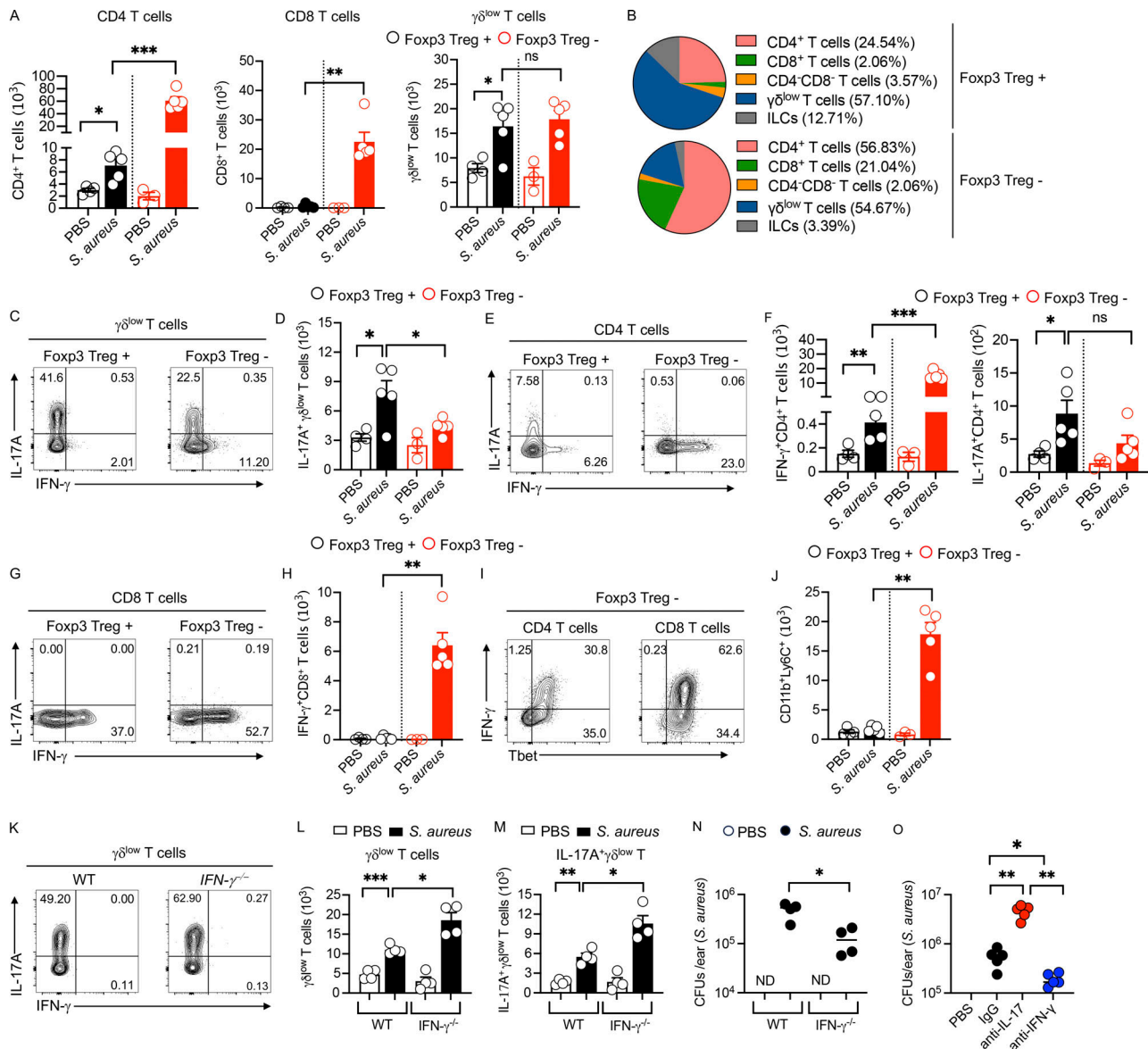
Figure 4. **Depletion of Foxp3⁺ Treg cells amplified type 1 immune responses.** C57BL/6 mice were colonized with a clinical *S. aureus* as in Fig. 1 A and euthanized on day 10 for ear skin collection and analysis. **(A)** Absolute numbers of CD4⁺ T, CD8⁺ T, and γδ^low T cells in Treg non-depleted (Foxp3⁺ Treg⁺) and Treg-depleted (Foxp3⁺ Treg⁻) Foxp3-DTR mice colonized with *S. aureus* or PBS control mice. Mean ± SEM representative of two experiments with three to five mice per group. **(B)** Pie chart showing percent contribution of T cells and ILCs in Treg non-depleted (Foxp3⁺ Treg⁺) and Treg-depleted (Foxp3⁺ Treg⁻) Foxp3-DTR mice colonized with *S. aureus*. Absolute numbers were used to create the chart. Two experiments with three to five mice per group. **(C)** IL-17A and IFN-γ production from γδ^low T cells in *S. aureus*–colonized, Treg-depleted (Foxp3⁺ Treg⁻) and non-depleted (Foxp3⁺ Treg⁺) Foxp3-DTR mice. Representative of two experiments with three to five mice per group. Numbers in contour plots indicate the percent of cells within the gates. **(D)** Absolute numbers of IL-17A⁺γδ^low T cells in PBS control and *S. aureus*–colonized, Treg-depleted (Foxp3⁺ Treg⁻) and non-depleted (Foxp3⁺ Treg⁺) Foxp3-DTR mice. Mean ± SEM representative of two experiments with three to five mice per group. **(E)** IL-17A and IFN-γ production from CD4⁺ T cells in *S. aureus*–colonized, Treg-depleted (Foxp3⁺ Treg⁻) and non-depleted (Foxp3⁺ Treg⁺) Foxp3-DTR mice. Representative of two experiments with three to five mice per group. Numbers in contour plots indicate the percent of cells within the gates. **(F)** Absolute numbers of IFN-γ⁺CD4⁺ T and IL-17A⁺CD4⁺ T in PBS control and *S. aureus*–colonized, Treg-depleted (Foxp3⁺ Treg⁻) and non-depleted (Foxp3⁺ Treg⁺) Foxp3-DTR mice. Mean ± SEM representative of two experiments with three to five mice per group. **(G)** IL-17A and IFN-γ production from CD8⁺ T cells in *S. aureus*–colonized, Treg-depleted (Foxp3⁺ Treg⁻) and non-depleted (Foxp3⁺ Treg⁺) Foxp3-DTR mice. Representative of two experiments with three to five mice per group. Numbers in contour plots indicate the percent of cells within the gates. **(H)** Absolute numbers of IFN-γ⁺CD8⁺ T in PBS control and *S. aureus*–colonized, Treg-depleted (Foxp3⁺ Treg⁻) and non-depleted (Foxp3⁺ Treg⁺) Foxp3-DTR mice. Mean ± SEM representative of two experiments with three to five mice per group. **(I)** T-bet expression in IFN-γ⁺CD4 and IFN-γ⁺CD8 T cells in *S. aureus*–colonized, Treg-depleted (Foxp3⁺ Treg⁻) Foxp3-DTR mice. Representative of two experiments with three to five mice per group. Numbers in contour plots indicate the percent of cells within the gates. **(J)** Absolute numbers of monocytes (CD11b⁺Ly6C⁺) by flow cytometry in Treg non-depleted (Foxp3⁺ Treg⁺) and -depleted (Foxp3⁺ Treg⁻) Foxp3-DTR mice colonized with *S. aureus* or non-colonized PBS control mice. Mean ± SEM representative of two experiments with three to five mice per group. **(K)** Flow cytometry analysis of IL-17A and IFN-γ production from γδ^low T cells in uncolonized (PBS, control) and *S. aureus*–colonized wild-type and IFN-γ⁻/⁻ mice at day 10. Representative of two experiments with four mice per group. Numbers in contour plots indicate the percent of cells within the gates. **(L and M)** Absolute numbers of γδ^low T cells and IL-17A⁺γδ^low T cells in uncolonized (PBS, control) and *S. aureus*–colonized wild-type and IFN-γ⁻/⁻ mice at day 10. Mean ± SEM

representative of two experiments with four mice per group. **(N)** CFUs of *S. aureus* in the ear skin of control (PBS) and *S. aureus*–treated WT and IFN-γ⁻/⁻ mice at day 10. Mean ± SEM representative of two experiments with three mice per group. **(O)** CFUs of *S. aureus* in the ear skin of control (PBS), IgG, anti–IL-17, and anti–IFN-γ treated mice. Wild-type mice were colonized with *S. aureus* at days 1–4 and killed on day 10 for analysis. Injection of anti–IL-17A or anti–IFN-γ was performed on days 0, 2, 4, and 7. From two experiments with five mice per group. *P < 0.05, **P < 0.01, and ***P < 0.001. "ns" denotes not significant. Significant P values by two-tailed unpaired Student's *t* test with Welch's correction are indicated in the figure.

skin compared with control mice (Fig. 6 A). To determine if the Tregs controlling the pathogenic type 1 response were RORγt⁺, we generated mice that lacked RORγt in Foxp3⁺ Treg cells and colonized them with *S. aureus* (Fig. 6 B). Similar to total depletion of Foxp3⁺ Tregs, the number of CD4 T cells, CD8 T cells, and monocytes were increased in Foxp3^Cre RORγt^fl/fl mice compared with RORγt^fl/fl mice after *S. aureus* colonization (Fig. S3 A). Further, after *S. aureus* colonization, mice that lack RORγt in Foxp3⁺ Tregs produced high levels of IFN-γ from CD4 T and CD8 T cells in the skin compared with mice that express RORγt in Foxp3⁺ Tregs (Fig. 6, C–F; and Fig. S3 B). In contrast, IL-17 production from CD4 T cells and γδ^low T cells was significantly decreased in Foxp3^Cre RORγt^fl/fl compared with RORγt^fl/fl mice (Fig. 6, C–E, G, and H; and Fig. S3 C). We found that RORγt deletion did not induce IL-17A or IFN-γ in Foxp3^YFP+ Tregs or change the number of Foxp3⁺ Treg cells after *S. aureus* colonization (Fig. S3, D–F). Our results are in contrast to the deletion of RORγt in colonic Foxp3⁺ Treg cells, which led to the production of inflammatory cytokines (Bhaumik et al., 2021). Similar to the results we observed in complete Treg depletion, mice that lack RORγt in Foxp3⁺ Treg cells developed significantly greater skin inflammation and histological alterations compared to mice that expressed RORγt in Tregs after *S. aureus* colonization (Fig. 6, I and J). We also observed a higher *S. aureus* burden on the skin of Foxp3^Cre RORγt^fl/fl compared with RORγt^fl/fl mice (Fig. 6 K). These results suggest that RORγt expression in Tregs is essential in regulating the IFN-γ from effector T cells in skin colonized with *S. aureus*.

Chronic reduction of Foxp3⁺ Treg cells promotes increased disease severity and S. aureus colonization in cutaneous leishmaniasis

Based upon the preceding findings, we hypothesized that a reduction in Tregs would promote increased IFN-γ–associated pathology and higher levels of *S. aureus* in cutaneous leishmaniasis. Since chronic depletion of all Tregs in mice leads to autoimmunity (Hu et al., 2021; Kim et al., 2007), we utilized female heterozygous Foxp3-DTR mice that contain one copy of DTR transgene and one copy of the normal endogenous Foxp3 allele. In these heterozygous Foxp3-DTR (Foxp3-DTR⁺/⁻) mice, only ∼50% of the Foxp3⁺ Treg cells are subjected to DT-mediated depletion (Kalekar et al., 2019). We topically colonized the mice with *S. aureus* as before, infected them with *L. braziliensis* on day 10, and treated them with DT once a week for 5 wk. We found that both lesion size and the pathology in *S. aureus*–colonized mice infected with *L. braziliensis* were significantly increased after the reduction of Tregs compared with all other groups, without any changes in the parasite burden (Fig. 7, A–C). Similarly, assessment of histological sections and flow cytometry analysis revealed that epidermal damage and infiltration of cell

infiltrates were increased in *L. braziliensis*–infected and *S. aureus*–colonized mice after the reduction of Tregs (Fig. 7 D and Fig. S4). While we could not deplete IFN-γ due to its role in controlling the parasites, we found that IFN-γ–producing αβ T cells in *S. aureus*–colonized mice infected with *L. braziliensis* were increased after reduction of Tregs compared with intact Tregs groups (Fig. 7 E). However, the mRNA transcripts of *Il17a* were decreased after reduction of Tregs compared with controls (Fig. 7 F). Finally, *S. aureus* levels were significantly higher in lesions when mice were partially depleted of Tregs (Fig. 7 G). Together, these results reveal a significant role for Tregs in moderating IFN-γ–mediated disease and opportunistic bacterial infection in cutaneous leishmaniasis.

Low FOXP3 expression is associated with enhanced IFNG, S. aureus abundance, and delayed healing in human cutaneous leishmaniasis

To assess the role of Tregs in human leishmaniasis, we took advantage of a whole transcriptome dual RNA sequencing (RNA-seq) dataset from lesion biopsies of *L. braziliensis*–infected patients (Amorim et al., 2023, *Preprint*). In this dataset, transcripts were mapped to the human transcriptome to estimate host gene expression and non-human transcripts were mapped to *S. aureus* to estimate *S. aureus* transcriptional abundances (Fig. 8 A). Using *FOXP3* as a unique marker for Treg cells (Fig. S5, A–C), we stratified the *L. braziliensis* lesions according to *FOXP3* expression into *FOXP3^high* and *FOXP3^low* groups (Fig. 8 B). To investigate whether the magnitude of *FOXP3* expression impacted the whole transcriptional gene expression patterns, we performed an unsupervised principal component analysis and found that *FOXP3^high* lesions presented distinct whole transcriptome profiles and clustered separately from *FOXP3^low* lesions, P < 0.01 (Fig. 8 C). We performed differential gene expression analyses between *FOXP3^low* and *FOXP3^high* lesions and observed a total of 136 genes overrepresented in *FOXP3^low* lesions. Included in this gene list were *IFNG* and genes encoding for cytolytic activity, such as *PRF1* and *GZMB*, which we have previously associated with treatment failure in *L. braziliensis* patients (Amorim et al., 2019). In the genes overrepresented in *FOXP3^high* lesions, Gene Ontology (GO) analysis revealed enrichment for responses to wounding, skin healing, and structural skin formation (Fig. 8 D and Fig. S5 D). Since our murine data suggested an association between Tregs, *S. aureus* colonization, and IFN-γ levels, we evaluated the association between *S. aureus*, *FOXP3*, and *IFNG* transcripts from the dual RNA-seq dataset. The samples were divided into *S. aureus*–high and *S. aureus*–low lesions based on a comparison with the quantities detected in healthy, intact skin samples (Fig. 8 E). The *S. aureus*–high lesions exhibited decreased *FOXP3* expression compared with the *S. aureus*–low lesions (Fig. 8 F), consistent with our murine studies suggesting that high levels of
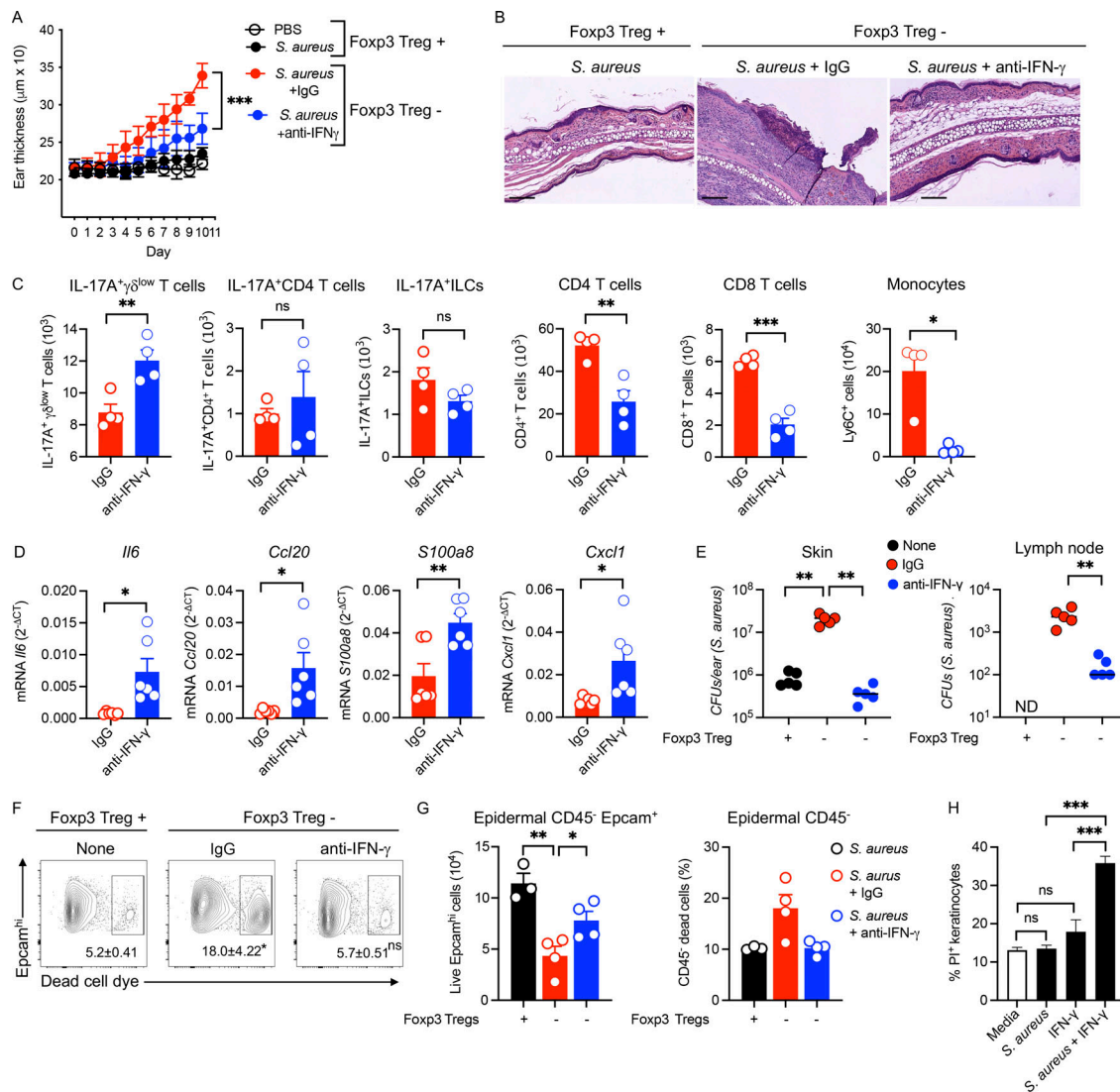
Figure 5. Excessive IFN- γ promotes inflammation, *S. aureus* growth, and barrier damage. (A) Ear thickness measurement in IgG or anti–IFN-γ treated PBS control and *S. aureus*–colonized, Treg-depleted (Foxp3⁺ Treg⁻) and non-depleted (Foxp3⁺ Treg⁺) Foxp3-DTR mice. Mice were colonized with *S. aureus* on days 1–4 and euthanized on day 10 for analysis. Injection of anti–IFN-γ was performed on days 0, 2, 4, and 7. DT was administered on days −1, 2, 4, and 6. Mean ± SD representative of two experiments with five mice per group. **(B)** H&E-stained sections of non-depleted (Foxp3⁺ Treg⁺) *S. aureus*–colonized mice or IgG or anti–IFN-γ treated *S. aureus*–colonized, Treg-depleted (Foxp3⁺ Treg⁻) Foxp3-DTR mice. Scale bar = 200 μm. **(C)** Absolute numbers of IL-17A⁺γδ^low T cells, IL-17A⁺CD4 T cells, IL-17A⁺ILCs, CD4 T cells, CD8 T cells, and CD11b⁺Ly6C⁺ monocytes in IgG or anti–IFN-γ treated *S. aureus*–colonized, Treg-depleted (Foxp3⁺ Treg⁻) Foxp3-DTR mice. Mean ± SEM representative of two experiments with four mice per group. **(D)** mRNA analysis of *Il6*, *Ccl20*, *S100a8*, and *Cxcl1* in the skin of IgG or anti–IFN-γ treated *S. aureus*–colonized, Treg-depleted (Foxp3⁺ Treg⁻) Foxp3-DTR mice. Mean ± SEM from two experiments with six mice per group. **(E)** CFUs of *S. aureus* in the ear skin and draining lymph node of non-depleted (Foxp3⁺ Treg⁺) *S. aureus*–colonized mice or IgG or anti–IFN-γ treated *S. aureus*–colonized, Treg-depleted (Foxp3⁺ Treg⁻) Foxp3-DTR mice. Representative of two experiments with five mice per group. **(F)** Analysis of Epcam⁺ dead epidermal cells by flow cytometry in the epidermis of non-depleted (Foxp3⁺ Treg⁺) *S. aureus*–colonized or IgG or anti–IFN-γ treated *S. aureus*–colonized, Treg-depleted (Foxp3⁺ Treg⁻) Foxp3-DTR mice. Cells gated on CD45⁻ cells from the epidermis. Representative of two experiments with three to four mice per group. Numbers in contour plots indicate the percent of cells within the gates. **(G)** Absolute numbers of live CD45⁻Epcam⁺ cells and CD45⁻ dead cells in the epidermis of IgG or anti–IFN-γ treated *S. aureus*–colonized, Foxp3⁺ Treg cells–depleted (Foxp3⁺ Treg⁻) and non-depleted (Foxp3⁺ Treg⁺) Foxp3-DTR mice. Mean ± SEM from two experiments with three to four mice per group. **(H)** Flow cytometry analysis of percent of propidium iodide (PI) positive human primary KCs were exposed to *S. aureus* for 18 h and then cultured with or without IFN-γ for 48 h at which time cells were collected for cytometric analysis. Mean ± SEM from two experiments with three to five mice per group. *P < 0.05, **P < 0.01, and ***P < 0.001. "ns" denotes not significant. Significant P values by two-tailed unpaired Student's *t* test with Welch's correction, except for H, which is one-way ANOVA with Tukey's multiple comparisons test, are indicated in the figure.

Tregs limit *S. aureus* infections in lesions. Also similar to murine studies, we found that *S. aureus*–high lesions had higher levels of *IFNG* transcripts (Fig. 8 F) and transcripts associated with cell killing/cytolysis (Fig. 8 G) than *S. aureus*–low lesions. Additionally, *S. aureus*–high lesions exhibited a decreased enrichment for

responses to wound healing (Fig. 8 G), similar to the enrichment for wound healing genes seen in *FOXP3* high-expressing lesions (Fig. 8 D). Finally, we investigated whether Tregs might influence the response to drug treatment in *L. braziliensis* patients. We utilized metadata associated with the RNA-seq
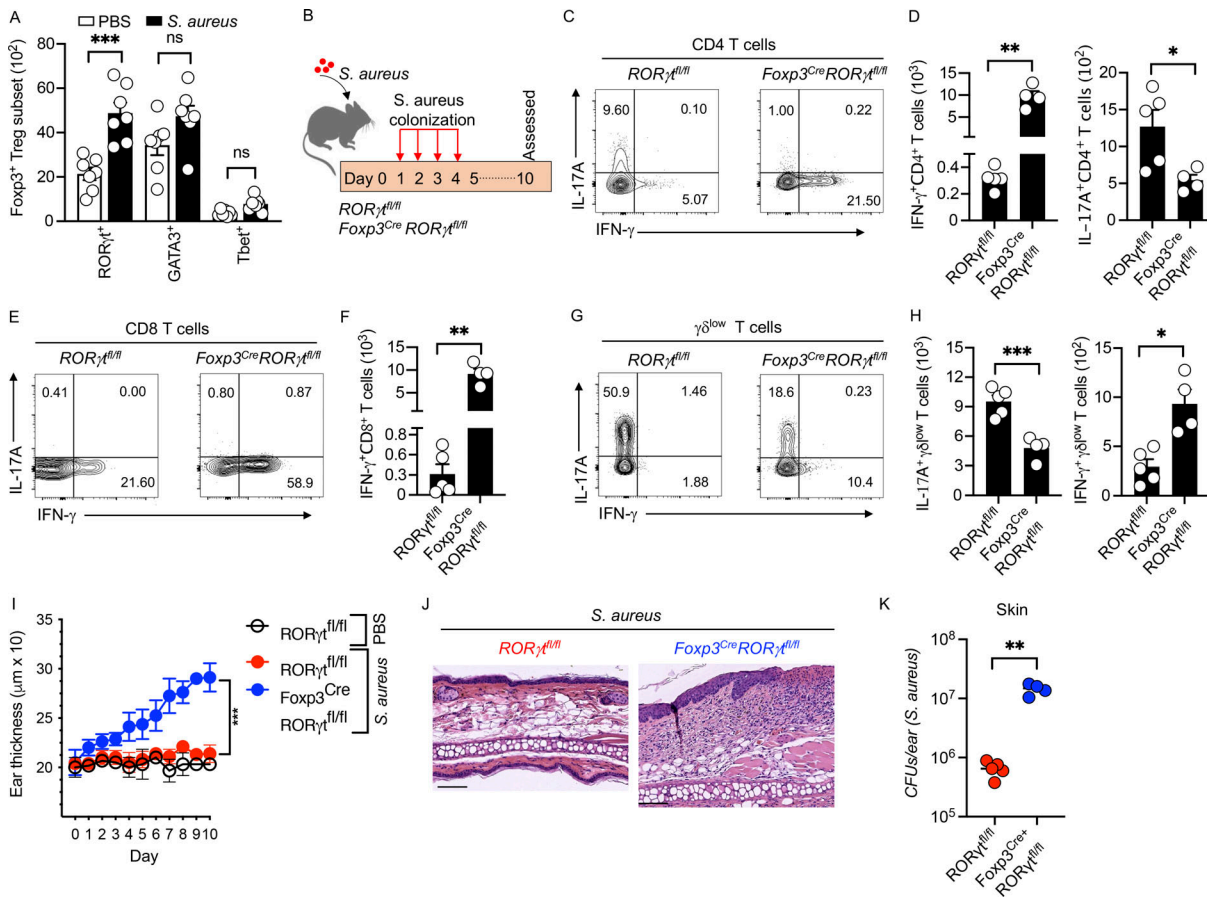
Figure 6. RORγt⁺Foxp3⁺ Tregs control type 1 immune responses. (A) Absolute numbers of Foxp3⁺ Tregs expressing the transcription factor RORγt, GATA3, or T-bet in PBS control and *S. aureus*–colonized mice. Wild-type mice were colonized with *S. aureus* on days 1–4 and euthanized on day 10 for analysis. Mean ± SEM from two experiments with seven mice per group. **(B)** Schematic representation of *S. aureus* colonization protocol in *RORγt^fl/fl* and *Foxp3^creRORγt^fl/fl* mice. Mice were colonized with *S. aureus* on days 1–4 and euthanized on day 10 for analysis. **(C)** Flow cytometry analysis of IL-17A and IFN-γ production from CD4⁺ T cells in *S. aureus*–colonized *RORγt^fl/fl* and *Foxp3^creRORγt^fl/fl* mice. Representative of two experiments with four to five mice per group. Numbers in contour plots indicate the percent of cells within the gates. **(D)** Absolute numbers of IFN-γ⁺CD4⁺ and IL-17A⁺CD4⁺ T cells in *S. aureus*–colonized *RORγt^fl/fl* and *Foxp3^creRORγt^fl/fl* mice. Mean ± SEM from two experiments with four to five mice per group. **(E)** Flow cytometry analysis of IL-17A and IFN-γ production from CD8⁺ T cells in *S. aureus*–colonized *RORγt^fl/fl* and *Foxp3^creRORγt^fl/fl* mice. Representative of two experiments with four to five mice per group. Numbers in contour plots indicate the percent of cells within the gates. **(F)** Absolute numbers of IFN-γ⁺CD8⁺ T cells in *S. aureus*–colonized *RORγt^fl/fl* and *Foxp3^creRORγt^fl/fl* mice. Mean ± SEM from two experiments with four to five mice per group. **(G)** Flow cytometry analysis of IL-17A and IFN-γ production from γδ^low T cells in *S. aureus*–colonized *RORγt^fl/fl* and *Foxp3^creRORγt^fl/fl* mice. Representative of two experiments with four to five mice per group. Numbers in contour plots indicate the percent of cells within the gates. **(H)** Absolute numbers of IL-17A⁺γδ^low T cells and IFN-γ⁺γδ^low T cells in *S. aureus*–colonized *RORγt^fl/fl* and *Foxp3^creRORγt^fl/fl* mice. Mean ± SEM from two experiments with four to five mice per group. **(I)** Ear thickness measurement of PBS control and *S. aureus*–colonized *RORγt^fl/fl* and *Foxp3^creRORγt^fl/fl* mice. **(J)** H&E-stained sections of *S. aureus*–colonized *RORγt^fl/fl* and *Foxp3^creRORγt^fl/fl* mice. Scale bar = 200 μm. Mean ± SD representative of two experiments with three to five mice per group. **(K)** CFUs of *S. aureus*–colonized *RORγt^fl/fl* and *Foxp3^creRORγt^fl/fl* mice on day 10. Mean ± SEM representative of two experiments with four to five mice per group. *P < 0.05, **P < 0.01, and ***P < 0.001. "ns" denotes not significant. Significant P values by two-tailed unpaired Student's *t* test with Welch's correction, except for A, which is one-way ANOVA with Tukey's multiple comparisons test, are indicated in the figure.

dataset (Amorim et al., 2023, *Preprint*) and assessed healing times in patients with high and low *FOXP3* transcripts. We found that patients with high *FOXP3* levels healed faster than those with low *FOXP3* levels (Fig. 8 H). These data suggest that, as in our mouse model, Tregs are critical in limiting pathologic levels of IFN-γ that promote tissue damage and *S. aureus* colonization in patients.

Discussion

The commensal microbiota provides signals that maintain skin function and integrity and promotes increased inflammation

when dysregulated. Using a combination of human and murine studies, we previously found that lesions associated with cutaneous leishmaniasis exhibited significant changes in the types and abundance of bacteria and found that these changes promote increased pathology (Gimblet et al., 2017). Here, colonizing mice with *S. aureus* isolates obtained from *L. braziliensis* patients, we show that Tregs moderate bacteria-induced pathologic responses and limit the abundance of *S. aureus*. Thus, in the absence of Tregs, mice developed a robust IFN-γ response that led to a skin barrier defect, increased cell death, decreased IL-17 responses, and invasion of *S. aureus* beyond the skin. Consistent with these murine studies, using an RNA-seq dataset of lesions
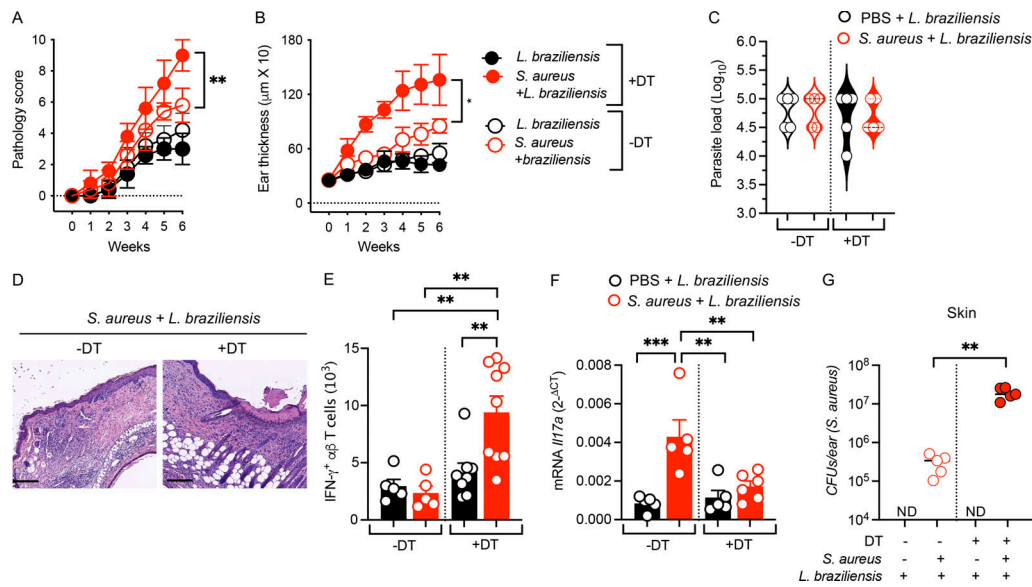
Figure 7. Impact of reduced Foxp3+ Tregs in *S. aureus*–colonized and *L. braziliensis*–infected mice. Foxp3-DTR heterozygous female mice were colonized on days 1–4 and then on day 10 (week 0). Mice were infected with *L. braziliensis* in one ear as in Fig. 2 A and euthanized at week 6 for analysis. Mice treated with DT at weeks 0, 1, 2, 3, 4, and 5 to chronically reduce the Foxp3+ Tregs. **(A and B)** Pathology score and change in ear skin thickness of different treatment groups of treated (+DT) and non-treated (−DT) Foxp3+DTR mice. Mean ± SD representative of two experiments with five mice per group. **(C)** Parasite load in *S. aureus* or PBS control mice infected with *L. braziliensis* and treated (+DT) or untreated (−DT) with DT. Representative of two experiments with five per group. **(D)** H&E-stained sections of ear skin of *S. aureus*–colonized and *L. braziliensis*–infected Foxp3-DTR heterozygous female mice treated (+DT) or untreated (−DT) with DT. **(E)** Absolute numbers of IFN-γ+αβ T cells in the ear skin of different treatment groups of treated (+DT) and untreated (−DT) with DT at week 6. Mean ± SEM from two experiments with five to nine mice per group. **(F)** mRNA analysis of *Il17a* in the ear skin of different treatment groups of treated (+DT) and untreated (−DT) with DT at week 6. Mean ± SEM from two experiments with five to six mice per group. **(G)** CFUs of *S. aureus* at week six in the ear of different treatment groups in treated (+DT) and untreated (−DT) mice. Representative of two experiments with five mice per group. *P < 0.05, **P < 0.01, and ***P < 0.001. "ND" denotes not detected. Significant P values by two-tailed unpaired Student's *t* test with Welch's correction, except for E and F, which are one-way ANOVA with Tukey's multiple comparisons test, are indicated in the figure.

from *L. braziliensis* patients (Amorim et al., 2023, *Preprint*), we found that low levels of *FOXP3* transcripts were associated with increased *S. aureus* colonization and a delay in lesion resolution. Thus, Tregs restrain type 1 immune responses in the skin to prevent epidermal damage and susceptibility to bacterial invasion.

The skin contains a plethora of microbes that can promote skin health but can also become pathogenic (Ansaldo et al., 2021; Flowers and Grice, 2020). Their role in several skin diseases, including psoriasis, atopic dermatitis, and wound healing, is well-studied (Alekseyenko et al., 2013; Byrd et al., 2017; Chang et al., 2018; De Francesco and Caruso, 2022; Fyhrquist et al., 2019; Geoghegan et al., 2018; Grice et al., 2010; Kobayashi et al., 2015; Liang et al., 2021; Liu et al., 2017). Still, we understand less about how microbes influence the outcome of skin infections such as cutaneous leishmaniasis. Our previous work and others found that a dysregulated skin microbiome develops in mice and people infected with *Leishmania* (Gimblet et al., 2017; Salgado et al., 2016). In mice, colonization with *Staphylococcus spp* leads to increased disease severity in cutaneous leishmaniasis, which is mediated by ILCs, γδ^{low} T cells, and Th17 cells (Gimblet et al., 2017; Naik et al., 2012; Singh et al., 2021). We recently found that *S. aureus* is a dominant member of the lesional microbiome in many *L. braziliensis* patients and that a high *S. aureus* burden was associated with delayed healing (Amorim et al., 2023, *Preprint*). Here, we show in a murine model that

S. aureus colonization induces an increase in IL-17 production that contributes to the control of skin colonizing bacteria but leads to more severe disease.

Since *S. aureus* colonization in mice led to an increase in Tregs, we investigated their role in the outcome of the infection. Tregs contribute to skin homeostasis, such as tissue repair, hair regeneration, and wound healing (Ali et al., 2017; Boothby et al., 2020; Mathur et al., 2019; Nosbaum et al., 2016), and their role in regulating unwanted immune responses is essential for survival (Kim et al., 2007). However, just as effector T cells are adaptable in the skin (Harrison et al., 2019), Tregs adapt to limit immune responses that are damaging to the integrity of the skin. For example, under homeostatic conditions, most Tregs in the skin express the transcription factor GATA3, and depletion of Tregs or GATA3 in Tregs leads to an increase in Th2 cytokines and dermal fibrosis (Harrison et al., 2019; Kalekar et al., 2019; Wohlfert et al., 2011). Similarly, in a model of allergic inflammation, RORα -expressing Tregs limited Th2 responses and skin inflammation in response to the vitamin D analog, calcipotriol (Malhotra et al., 2018). However, in response to tape stripping, Tregs blocked IL-17 responses and neutrophil recruitment, thereby promoting epidermal repair (Mathur et al., 2019), while when Tregs were depleted in a murine model of psoriasis, GM-CSF–producing CD4+ T cells dominated, rather than IL-17 responses (Hartwig et al., 2018). Similar to our results, Tregs can also limit IFN-γ responses in other situations. For example, in a
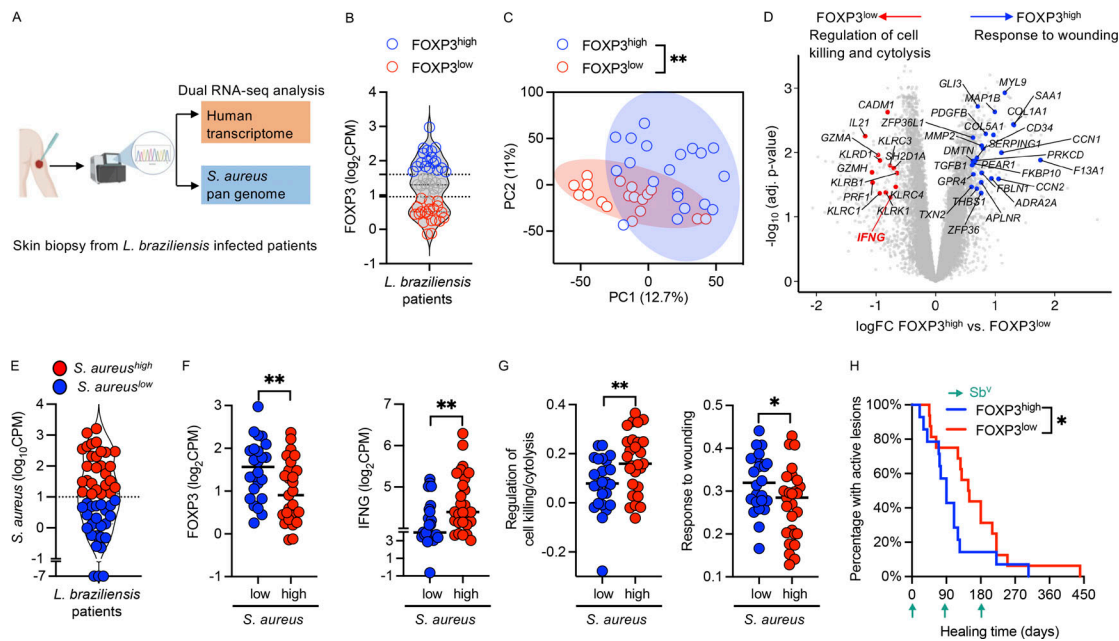
Figure 8. Reduced expression of *FOXP3* is associated with enhanced *IFNG* expression and *S. aureus* burden in human cutaneous leishmaniasis lesions. **(A)** Dual RNA-seq analyses were performed on lesion biopsies from *L. braziliensis*–infected patients. The transcripts were first mapped to the human transcriptome, and then unmapped transcripts were aligned to an in-house *S. aureus* pan-genome to estimate host gene expression and *S. aureus* transcriptional abundances, respectively. **(B)** *FOXP3* expression in the lesion biopsies. Lesions were subgrouped in *FOXP3*high- and *FOXP3*low-expressing lesions. Biopsies from 51 patients were used for analysis. Each dot represents a patient. **(C)** Principal component analysis of *FOXP3*high and *FOXP3*low samples. Data represent 19 *FOXP3*high- and 20 *FOXP3*low-expressing biopsies. **(D)** Differential gene expression analysis was performed between *FOXP3*high and *FOXP3*low samples. GO accessing biological process was conducted in the list of genes significantly enriched in each group, with cutoff thresholds of FC = 1.5 and adjusted P values = 0.05. Volcano plot with genes differentially expressed, highlighting genes annotated as "response to wounding" (blue) and "regulation of cell killing/cytolysis" (red) from GO analyses. **(E)** All lesion biopsies in the dataset were classified into two groups: *S. aureus*–high samples with higher bacterial transcriptional abundances relative to *S. aureus*–low samples that presented levels comparable to healthy skin. Biopsies from 51 patients were used for analysis. **(F and G)** *FOXP3* and *IFNG* expression (F), the "Regulation of cell killing/cytolysis" GO term score and the "response to wounding" GO term score (G) in *S. aureus*–high and *S. aureus*–low lesions. Data represent 24 *S. aureus*–low and 27 *S. aureus*–high expressing biopsies. Two-tailed unpaired Student's *t* test with Welch's correction. **(H)** Healing time for patients with *FOXP3*high- and *FOXP3*low-expressing lesions. Green arrows indicate the rounds for antimony treatment. Data represents 19 *FOXP3*high- and 20 *FOXP3*low-expressing biopsies. Gehan-Breslow-Wilcoxon test. *P < 0.05 and **P < 0.01.

skin wounding model, Treg depletion led to increased IFN-γ production, recruitment of CD11b+Ly6C+ myeloid cells, and delayed wound repair (Nosbaum et al., 2016). Paradoxically, in other situations, Tregs may be proinflammatory. For example, via a TGFβ-KC pathway, Tregs increase neutrophil recruitment, which may delay epidermal repair but simultaneously provide protection against bacteria in the skin (Moreau et al., 2021). Our studies found that Tregs promoted bacteria control by limiting IFN-γ, which at high levels promotes barrier disruption and blocks IL-17 responses. While T-bet–expressing Tregs are known to control type 1 immune responses (Di Giovangiulio et al., 2019; Koch et al., 2009), in our studies, the Tregs controlling the Th1 response expressed RORγt and may be similar to intestinal RORγt-expressing Tregs that develop in response to microbiota (Sefik et al., 2015).

We found that Treg depletion increased the amount of *S. aureus* in lesions, leading to *S. aureus* invasion into the dermis and draining lymph nodes. Our results indicate that the increase in *S. aureus* is due to the increase in IFN-γ, which downregulated an IL-17 response that controls bacteria (Cho et al., 2010). The inhibition of IL-17 by IFN-γ is consistent with previous studies showing that IFN-γ inhibits IL-17 production (Cruz et al., 2006; Harrington et al., 2005; Stumhofer et al., 2006). While other

studies have indicated that IFN-γ can control *S. aureus* (Brown et al., 2015), our results are more consistent with studies where IFN-γ was not protective against *S. aureus* (Montgomery et al., 2014; Tuffs et al., 2022). In addition to limiting IL-17 responses, the high levels of IFN-γ led to increased damage to the skin, which may further create an environment that favors *S. aureus* growth, and specifically allowed invasion of the bacteria beyond the skin barrier. A role for IFN-γ in skin damage is observed in other contexts. For example, high levels of IFN-γ promote KC cell death in chronic phases of inflammation (Hu and Ivashkiv, 2009) and drive Fas- and caspase-8–mediated KC cell death in toxic epidermal necrolysis (Viard-Leveugle et al., 2013). Type 1 responses are also associated with KC necroptosis in lichen planus and lupus erythematosus, and KCs of patients with atopic dermatitis show increased IFN-γ–induced apoptosis (Rebane et al., 2012; Shao et al., 2019; Trautmann et al., 2001). Further, a recent report suggests that excessive IFN-γ–dependent cell death leads to susceptibility to oral mucosal infection by the commensal fungus *Candida albicans* (Break et al., 2021). Thus, decreased IL-17 production and IFN-γ–mediated skin damage likely promote increased *S. aureus* levels. With the increased numbers of IFN-γ–producing cells in mice with fewer Tregs, one might predict that there would be better parasite control,

which was not the case. These results contrast with a study showing that depletion of Tregs in *Leishmania panamensis*–infected mice led to increased parasite numbers and larger lesions (Ehrlich et al., 2014). However, similar to our findings, Ehrlich et al. (2014) found that Treg depletion led to a substantial increase in IFN-γ. A possible explanation for this observation is that IL-10 from cells other than Tregs cells known to be induced in leishmaniasis may be blunting the effects of IFN-γ (Anderson et al., 2007; Bunn et al., 2018). Supporting this hypothesis, in experimental visceral leishmaniasis, depletion of Tregs had little influence on the parasite burden (Bunn et al., 2018). Indeed, Treg depletion in this study was not equivalent to IL-10 depletion, which we previously reported leads to an exaggerated IL-17 response (Gonzalez-Lombana et al., 2013). This could be due to the presence of *S. aureus* in our current study, a dose effect of IL-10, a role for non-pathogenic IL-10–producing Th17 cells, or an IL-10–independent function of Tregs in the skin. We are currently evaluating each of these possibilities.

One limitation of these studies is that we cannot differentiate between the depletion of Tregs in the skin and systemically in our murine experiments. There is no straightforward approach to specifically delete Tregs in the skin. However, while not negating a possible influence of systemic Tregs in leishmaniasis, our transcriptional studies on lesions from patients suggest that the number of Tregs in the lesions affects healing. The variability we find in transcripts for *FOXP3* in lesions is consistent with previous studies of Tregs, indicating that there is variability in the number of Tregs in leishmanial lesions (Barros et al., 2018; Belkaid et al., 2002; Campanelli et al., 2006; Costa et al., 2013; Mendez et al., 2004; Rodriguez-Pinto et al., 2012; Falcão et al., 2012). What drives that variability is unknown.

Regulation of unwanted immune responses is critical in skin diseases, and Tregs play a large role in that regulation. Here, we show that in the context of *S. aureus*, Tregs limit IFN-γ responses, leaving intact bacteria-protective IL-17 responses. While IL-17 promotes inflammation in the skin, the IL-17 response is less damaging as it avoids a more severe inflammation caused by high levels of IFN-γ leading to increased epidermal cell death, barrier breach, and increased levels of *S. aureus*. Our data suggest that the number of Tregs in leishmanial lesions will significantly impact the immune response, the bacterial burden, and the disease outcome, suggesting that in other contexts, variable numbers of Tregs may play a similar role. Thus, our findings show that Tregs not only limit immune responses but also modulate the type of immune responses that dominate and, in the context of an altered microbiome, can act as guardians against overwhelming bacterial infections.

Materials and methods
Study design
The objective of this study was to determine the role of Foxp3 Tregs in controlling the impact of *S. aureus* colonization in cutaneous leishmaniasis. To achieve this objective, we used clinical *S. aureus* isolates from *L. braziliensis* patients and designed and performed experiments using cellular and molecular immunology, microbiology, and bioinformatic techniques. We performed flow cytometry, quantitative PCR, cytokine analysis, cell culture,

RNA-seq analysis, bacterial and parasite culture, and murine in vivo infection and inflammation models. The sample size and number of independent experiments and statistical analysis are indicated in each figure legend.

Ethics statement
All animals were used in accordance with the recommendations in the Guide for the Care and Use of Laboratory Animals of the National Institutes of Health, and the guidelines of the University of Pennsylvania Institutional Animal Use and Care Committee. The protocol was approved by the Institutional Animal Care and Use Committee, University of Pennsylvania Animal Welfare Assurance Number D16-00045 (A3079-01). This study was conducted according to the principles specified in the Declaration of Helsinki and under local ethical guidelines (Ethical Committee of the Faculdade de Medicina da Bahia, Universidade Federal da Bahia, Salvador, Bahia, Brazil, and the University of Pennsylvania Institutional Review Board), and all patients signed informed consent before enrollment into the study.

Mice
Age-matched male wild-type C57BL/6 mice were purchased from Charles River Laboratories or from Jackson Laboratory. *Foxp3^DTR* (B6.129(Cg)-Foxp3tm3(DTR/GFP)Ayr/J [https://www.jax.org/strain/016958]), *Foxp3^YFP/Cre* (B6.129(Cg)-Foxp3tm4(YFP/icre)Ayr/J [https://www.jax.org/strain/016959]), *RORγt^fl/fl* (B6(Cg)-Rorctm3Litt/J [https://www.jax.org/strain/008771]), and *IFN-γR^−/−* (B6.129S7-Ifngr1tm1Agt/J [https://www.jax.org/strain/003288]) were purchased from The Jackson Laboratory. IFN-γ^−/− mice were a gift from C. Hunter (University of Pennsylvania, Philadelphia, PA, USA). Littermates were used for the *Foxp3^DTR* (B6.129(Cg)-Foxp3tm3(DTR/GFP)Ayr/J [https://www.jax.org/strain/016958]) mice and the *RORγt^fl/fl* (B6(Cg)-Rorctm3Litt/J [https://www.jax.org/strain/008771]) mice. Wild-type C57BL/6 mice were used as controls for the IFN-γ^−/− mice. All mice were maintained in specific pathogen–free facilities at the University of Pennsylvania. Mice were randomly assigned to experimental groups, were 6–8 wk old at the start of the experiment, and were age-matched within each experiment.

S. aureus isolation and identification
Human isolates of *S. aureus* were taken from the skin of *L. braziliensis* patients. Bacterial swabs were collected topically from the lesions of human subjects with cutaneous leishmaniasis from Brazil and stored in cryotubes with freezing media (autoclaved, filtered tryptic soy broth [TSB] dissolved in deionized water with 1% sterile Tween 80% and 15% glycerol) at −20°C. For bacterial identification, swabs were removed from TSB and streaked out onto blood agar plates (trypticase soy agar with Sheep Blood Plate; R01201; Remel) overnight at 37°C. Bacterial species were identified using Matrix-assisted laser desorption/ionization-time of flight at the Pennsylvania Animal Diagnostic Laboratory System, New Bolton Center.

S. aureus colonization and CFU quantification
S. aureus was cultured in TSB for 24 h at 37°C in a shaking incubator. After centrifugation, bacterial pellets were suspended

Singh et al.
Treg control of *S. aureus* in leishmaniasis

Journal of Experimental Medicine 13 of 19
https://doi.org/10.1084/jem.20230558

in TSB. Mice were topically associated by applying up to 300 μl of suspended bacteria (10^8–10^9 CFUs) to the ears and back of the mouse using sterile cotton swabs, every day for a total of 4 d to colonize mice. For total bacteria quantification, serially diluted digested ears were plated on blood agar plates and incubated overnight at 37°C. For *S. aureus* quantification, serially diluted samples were plated on CHROMagar *S. aureus* selective medium plates.

L. braziliensis infection

L. braziliensis parasites (strain MHOM/BR/01/BA788) were grown in Schneider's *Drosophila* medium (Gibco BRL) supplemented with 20% heat-inactivated fetal bovine serum (FBS; Invitrogen) and 2 mM L-glutamine for 6–7 d. The infectious metacyclic promastigotes of *L. braziliensis* were isolated by Ficoll (Sigma-Aldrich) density gradient centrifugation (Späth and Beverley, 2001). Mice were inoculated intradermally in the ear with 20 μl PBS containing $1 × 10^6$ *L. braziliensis* parasites. Lesion development was monitored by a pathology score and ear thickness measurement as described (Singh et al., 2021). In brief, pathology scores were assessed using the following inflammatory features: swelling/redness, deformation, ulceration, and loss of tissue. Each feature was scored as no symptom (0), mild (1), moderate (2), and severe (3) of individual mice. The scores were summed, resulting in a maximal score of 12. Parasite burden in lesion tissues was assessed using a limiting dilution assay.

TLR7-L (imiquimod) treatment

To induce dermatitis, mice were topically treated with imiquimod, a TLR7-L ligand that induces IL-23/IL-17–dependent skin inflammation. Mice were treated with TLR7-L on days 10, 11, and 12 after *S. aureus* colonization on days 1–4 as described above. TLR7-L (5% imiquimod; 3M Health Care Limited) was topically applied with a sterile plastic applicator on both sides of either ear of a mouse (Liu et al., 2022).

DT treatment in Foxp3-DTR mice

Foxp3$^+$ Tregs were depleted in Foxp3-DTR mice by DT treatment. Mice were injected with 15 ng/g body weight on day −1 and then on days 2, 4, and 6 to transiently deplete the Foxp3$^+$ Treg cells as described (Ali et al., 2017). On day 10, mice were killed to harvest the tissue for analysis. To chronically reduce the Foxp3$^+$ Tregs in *L. braziliensis* infection model, female heterozygous Foxp3-DTR/WT mice were injected with 15 ng/g body weight at week 0 and then at weeks 1, 2, 3, 4, and 5 (Ali et al., 2017; Kalekar et al., 2019).

Neutralization of IL-17A and IFN-γ

WT mice were injected i.p. with 500 μg anti–IL-17A antibody (17F3; BioXCell) or anti–IFN-γ antibody (XMG 1.2; BioXCell). Mouse IgG1 was used as an isotype control (MOPC-21; BioXcell). In both cases, mice were injected 1 d before the start of the *S. aureus* colonization at day 0 and then at days 2, 4, and 7. To study the IFN-γ–mediated tissue damage and inflammation in the absence of Foxp3$^+$ Tregs, FoxP3-DTR mice were injected with 500 μg anti–IFN-γ antibody 1 d before the start of the *S. aureus*

colonization at day 0 and then at days 2, 4, and 7 during the DT treatment protocol.

Hematoxylin and eosin (H&E) histology

Mice were sacrificed at different time points and the ear skin was fixed in 10% paraformaldehyde. Paraffin-embedded sections were cut and stained with H&E for analysis. H&E staining was performed by the Comparative Pathology Core at Penn Vet, University of Pennsylvania.

RNA isolation and quantitative RT-PCR (qRT-PCR)

Ear tissue was stored in RNAlater solution and total RNA was extracted using the RNeasy Fibrous Tissue Mini Kit (Qiagen) according to the manufacturer's instructions. For mRNA transcript analysis, real-time PCR was performed using SuperScript One Step RT-PCR (PCR with reverse transcription) kit (Invitrogen). Fluorescein amidite–labeled primers and probes were purchased from Applied Biosystems/Thermo Fisher Scientific to quantify the gene expression. Gapdh (Mm99999915_g1), *Ifng* (Mm01168134_m1), *Il3* (Mm00434204_m1), *Il17a* (Mm00439618_m1), *Il6* (Mm00446190_m1), *Ccl20* (Mm01268754_m1), *S100a8* (Mm00496696_g1), and *Cxcl1* (Mm04207460_m1) were used for analysis. The reactions were run on an Applied Biosystems ViiA 7 Real-Time PCR system using the standard protocol provided by Invitrogen. The expression of mRNAs was normalized to Gapdh mRNA by calculating $2^{-\Delta Ct}$. The threshold cycle at the limit of detection for cytokine mRNAs was 40, which was used for calculating $2^{-\Delta Ct}$ in the case of undetectable cycles by qRT-PCR.

Cytokine and chemokine array analysis

To quantify the cytokines and chemokines in *S. aureus*–colonized skin, we performed array analysis on the extracted total RNA using RT^2 Profiler PCR Array Mouse Cytokines & Chemokines (PAMM-150ZE-4; Qiagen). The reaction was performed using SuperScript III Platinum SYBR Green One-Step qRT-PCR (PCR with reverse transcription) kit (Invitrogen). The expression of mRNAs was normalized to the reference gene Gusb and reference sample PBS control by calculating $2^{-\Delta\Delta Ct}$. Gene expression values were represented as fold change, which is $2^{-\Delta\Delta Ct}$. $\Delta CT = CT$(a target gene) − CT(a reference gene). $\Delta\Delta CT = \Delta CT$(a target sample) − ΔCT(a reference sample).

Tissue processing and flow cytometry analysis

To prepare single-cell suspensions, ventral and dorsal sheets of the ear were separated from the cartilage and incubated for 90 min in CO_2 incubator at 37°C in 1 ml volume of RPMI 1640 (Invitrogen) containing 0.25 mg ml^{-1} liberase TL (Roche Diagnostics). The digested ears were passed through a 3-ml syringe to make single-cell suspension. After disruption with a syringe, the reaction was stopped by adding cold 1 ml FACS buffer containing 2% FBS and 0.5 mM EDTA. The lymph nodes were mechanically disrupted using a syringe plunger in cold FACS buffer. The cells were filtered through 70-μm nylon mesh and washed in FACS buffer at 1,500 rpm for 5 min. Cells were suspended in FACS buffer for further analysis. For surface staining, the following antibodies were used at 1:100 dilutions in FACS buffer according to the manufacturer's specifications.

CD45 (30-F11; eBiosciences), CD3 (17A2; eBiosciences), CD90.2 (53-2.1; eBiosciences), γδTCR (GL3; eBiosciences), βTCR (H57-597; eBiosciences), CD4 (RM4-5; BioLegend), CD8 (YTS5167.7; eBiosciences), CD25 (PC61.5; eBiosciences), ST2 (D1H9; BioLegend), CD11b (M1/70; eBiosciences), Ly6G (1A8; eBiosciences), Ly6C (AL-21; BD Pharmingen), Epcam (G8.8; BioLegend), and dead cell marker. For counting the cells, AccuCount Fluorescent particles (Spherotech) were used. The stained cells were run on an LSR-II flow cytometer (BD Biosciences) and the acquired data were analyzed using FlowJo software (Tree Star).

Intracellular cytokine and transcription factors staining
For intracellular cytokine staining, cells were incubated for 4 h with leukocyte-activating cocktail (BD Biosciences) in DMEM containing 2 mM L-glutamine (Invitrogen) in a CO_2 incubator at 37°C. After activation, cells were washed with FACS buffer at 1,500 rpm for 5 min. Following surface staining, the cells were fixed for 60 min and then permeabilized using the BD Cytofix/Cytoperm Plus Kit (BD Biosciences). Subsequently, permeabilized cells were stained overnight with anti–IL-17A (TC11-18H10; BD Pharmingen), anti–IFN-γ (XMG 1.2; eBiosciences), IL-10 (JES5-16E3; BD Pharmingen), GM-CSF (MP-22E9; BioLegend), IL-22 (Poly4164; BioLegend), and TNF-α (MP1-22E9; BioLegend). For Ki67 (SolA15; eBiosciences) analysis, cells were incubated for 1 h. To stain transcription factors, after surface staining, cells were fixed for 90 min and then permeabilized using Foxp3/transcription factor staining kit (eBiosciences) according to the manufacturer's instructions. Cells were stained overnight with Foxp3 (FJK-16s; eBiosciences), RORγt (B2D; Invitrogen), GATA3 (L50-823; BD Horizon), T-bet (O4-46; BD Horizon), ICOS (C398.4A; BD Biosciences), and CD152 (AFS98; eBiosciences). The analysis of cells by flow cytometry was done as described above.

Human primary KC culture and stimulation
To determine the effect S. aureus and IFN-γ exposure on human KCs, we cultured the primary human KCs obtained from the Skin Biology and Diseases Resource Center, Penn Dermatology in KC Media 2 supplemented with 0.06 mM CaCl2 and SupplementalMix (C-20011; Promo Cell). Cells were seeded at 10^5 per well in 6-well plates. At 75% confluency, cells were fed with fresh media and exposed to 10^6 S. aureus in 2 ml total media. After 18 h, cells were stimulated with 50 ng/ml IFN-γ for 48 h. Cells were detached using Cell Detachment Kit (C-41000; Promo Cell) to stain with propidium iodide and flow cytometry analysis.

Single-cell RNA-seq analysis
To identify the Treg-specific gene expression footprint (gene biomarkers), we reanalyzed an integrated publicly available single-cell RNA-seq dataset in the format of a Seurat R object. In this study, CD45+ cells were collected from the skin of healthy subjects and from the affected skin of patients with psoriasis vulgaris, atopic dermatitis, lichen planus, bullous pemphigoid, and indeterminate rashes for sequencing (Liu et al., 2022). The R objects associated with this dataset were downloaded from Zenodo #6470377 (https://zenodo.org/record/6470377#.Y1gAa-zMIUH). The four previously classified Treg subpopulations

(eTreg1 + Treg-c + cmTreg + eTreg2) were combined into one general Treg cluster, and a differential gene expression analysis between the Treg cluster and all the non-Treg clusters combined was performed with cutoff thresholds of fold change (FC) ≥ 2 and P < 0.0001. FOXP3 was defined as a unique and exclusive gene biomarker associated with Treg classification in the skin of human subjects. All analyses and visualizations were carried out using the statistical computing environment R version 4.2.1, R Studio version 2022.02.3 build 492, and Bioconductor version 3.15. Single-cell RNA-seq analyses were performed using the Seurat R package. The tidyverse suite of R packages and GraphPad Prism were used in combination for data visualization. Differential gene expression analyses with Benjamini-Hochberg correction for multiple testing were carried out using the Limma R package.

Bulk RNA-seq analysis
To evaluate the impact of the magnitude of Treg (FOXP3) gene expression in the whole-lesional transcriptome in human cutaneous leishmaniasis, we analyzed RNA-seq on 51 biopsies from skin lesions of L. braziliensis patients, available at Gene Expression Omnibus accession no. GSE214397, in a format of filtered, normalized gene versus sample matrix. FOXP3low and FOXP3high lesions were defined based on the distribution of samples expressing FOXP3. For further analysis, only FOXP3low (N = 20) and FOXP3high (N = 19) expressing samples were used. Principal component analysis was performed with the prcomp R package, where ellipses were drawn with a 95% interval confidence. The non-parametric multivariate statistical permutation test was used for statistical significance differences between FOXP3low versus FOXP3high lesion whole transcriptomes using the vegan R package. The Gehan-Breslow-Wilcoxon test was used for statistical significance in healing time survival curves. GO analysis was done with Metascape (http://metascape.org) using the gene list from FOXP3low and FOXP3high lesions. Single sample gene set enrichment analysis was used to calculate the "response to wounding" and the "cell killing/cytolysis" enrichment scores per lesion sample with the gene set variation analysis package. The immunedeconv package was used to estimate cell abundances from bulk RNA-seq data using the Microenvironment Cell Populations-counter method12. The non-parametric tests Spearman and Mann-Whitney were used to compare two-group cases and correlations, respectively. In all statistical testing, *P < 0.05, **P < 0.01, and ***P < 0.001.

S. aureus transcript abundance analysis in lesions from cutaneous leishmaniasis patients
The S. aureus transcriptional abundances in each lesion biopsy were quantified by performing dual RNA-seq analysis, mapping non-human transcripts using KneadData to an in-house S. aureus pangenome. This S. aureus pangenome was composed of whole genome sequences of S. aureus isolated from the lesions of L. braziliensis patients and publicly available S. aureus genome (Amorim et al., 2023, Preprint). All the 51 samples included in this dataset were characterized by either S. aureus–positive samples or S. aureus–low samples, with the

cutoff based on abundances of *S. aureus* transcripts in healthy, intact skin.

Statistical analysis

In each experiment, mice were randomly assigned to the treatment groups and the number of mice per group used in an experiment is shown in the corresponding figure legend. Two-tailed unpaired Student's *t* test with Welch's correction or one-way analysis of variance (ANOVA) was performed for significance. The mean is represented as the standard error of the mean (SEM) or standard deviation (SD) as shown in each figure legend. For comparing the same samples/groups at different time points, SD was used to represent the mean. P value <0.05 is considered as significant.

Online supplemental material

Fig. S1 shows characterization of IL-17 phenotype including gating strategy to analyze T cells and ILCs and IL-17A and IFN-γ production from these cells, mRNA analysis of cytokine and chemokines in the skin of *S. aureus*–colonized mice and histology. Ear thickness and *S. aureus* load in the skin after anti–IL-17 treatment in *S. aureus*–colonized mice infected with *L. braziliensis*. Fig. S2 shows Foxp3 expression in different cell types, IL-10 production from Foxp3 Tregs, Foxp3 Tregs in IFN-γ–deficient mice, and additional data on impact of Foxp3 Treg depletion on cytokine production from T cells. Fig. S3 shows additional data of Foxp3^{Cre} RORgt$^{fl/fl}$ mice. Fig. S4 shows inflammatory cell infiltrate in DT-treated and non-treated *L. braziliensis* infection model colonized with *S. aureus*. Fig. S5 shows validation of *FOXP3* gene as a unique marker of Treg by analyzing single-cell sequencing data and GO terms enrichment pathway analysis of genes associated with *FOXP3*^{high} and *FOXP3*^{low} by using Metascape Pathway analysis tool. Four tables are provided online. Table S1 provides differential gene expression between *FOXP3*^{high} versus *FOXP3*^{low} samples. Table S2 provides a gene list for GO analysis using Metascape associated with *FOXP3*^{high} versus *FOXP3*^{low}. Table S3 provides Metascape results for *FOXP3*^{high} gene list. Table S4 provides Metascape results for *FOXP3*^{low} gene list.

Data availability

The raw sequence data from the bulk RNA-seq of lesions from cutaneous leishmaniasis patients is available at Gene Expression Omnibus BioProject PRJNA885131. The whole genome sequencing for *S. aureus* clinical isolates is available at Sequence Read Archive BioProject PRJNA922957. The single-cell RNA-seq of skin of patients with skin diseases is available at the European Genome-Phenome Archive EGAS00001005271. The main R scripts used to perform the computational analyses in sequencing datasets have been archived on Zenodo and are available in Github (https://github.com/camilafarias112/Tregs_Singh2023).

References

Alekseyenko, A.V., G.I. Perez-Perez, A. De Souza, B. Strober, Z. Gao, M. Bihan, K. Li, B.A. Methé, and M.J. Blaser. 2013. Community differentiation of the cutaneous microbiota in psoriasis. *Microbiome*. 1:31. https://doi.org/10.1186/2049-2618-1-31

Ali, N., B. Zirak, R.S. Rodriguez, M.L. Pauli, H.A. Truong, K. Lai, R. Ahn, K. Corbin, M.M. Lowe, T.C. Scharschmidt, et al. 2017. Regulatory T cells in skin facilitate epithelial stem cell differentiation. *Cell*. 169:1119–1129.e11. https://doi.org/10.1016/j.cell.2017.05.002

Amorim, C.F., F.O. Novais, B.T. Nguyen, A.M. Misic, L.P. Carvalho, E.M. Carvalho, D.P. Beiting, and P. Scott. 2019. Variable gene expression and parasite load predict treatment outcome in cutaneous leishmaniasis. *Sci. Transl. Med.* 11:eaax4204. https://doi.org/10.1126/scitranslmed.aax4204

Amorim, C.F., V.M. Lovins, T.P. Singh, F.O. Novais, J.C. Harris, A.S. Lago, L.P. Carvalho, D.P. Beiting, P. Scott, and E.A. Grice. 2023. The skin microbiome enhances disease through IL-1b and delays healing in cutaneous leishmaniasis patients. *medRxiv*. https://doi.org/10.1101/2023.02.02.23285247 (Preprint posted February 07, 2023).

Anderson, C.F., M. Oukka, V.J. Kuchroo, and D. Sacks. 2007. CD4(+)CD25(−)Foxp3(−) Th1 cells are the source of IL-10-mediated immune suppression in chronic cutaneous leishmaniasis. *J. Exp. Med.* 204:285–297. https://doi.org/10.1084/jem.20061886

Ansaldo, E., T.K. Farley, and Y. Belkaid. 2021. Control of immunity by the microbiota. *Annu. Rev. Immunol.* 39:449–479. https://doi.org/10.1146/annurev-immunol-093019-112348

Barros, N., N. Vasquez, F. Woll, C. Sanchez, B. Valencia, A. Llanos-Cuentas, A.C. White Jr, and M. Montes. 2018. Regulatory T-cell dynamics in cutaneous and mucocutaneous leishmaniasis due to *Leishmania braziliensis*. *Am. J. Trop. Med. Hyg.* 98:753–758. https://doi.org/10.4269/ajtmh.17-0624

Belkaid, Y., C.A. Piccirillo, S. Mendez, E.M. Shevach, and D.L. Sacks. 2002. CD4+CD25+ regulatory T cells control Leishmania major persistence and immunity. *Nature*. 420:502–507. https://doi.org/10.1038/nature01152

Bhaumik, S., M.E. Mickael, M. Moran, M. Spell, and R. Basu. 2021. RORγt promotes Foxp3 expression by antagonizing the effector program in colonic regulatory T cells. *J. Immunol.* 207:2027–2038. https://doi.org/10.4049/jimmunol.2100175

Boaventura, V.S., C.S. Santos, C.R. Cardoso, J. de Andrade, W.L.C. Dos Santos, J. Clarêncio, J.S. Silva, V.M. Borges, M. Barral-Netto, C.I. Brodskyn, and A. Barral. 2010. Human mucosal leishmaniasis: Neutrophils infiltrate areas of tissue damage that express high levels of Th17-related cytokines. *Eur. J. Immunol.* 40:2830–2836. https://doi.org/10.1002/eji.200940115

Boothby, I.C., J.N. Cohen, and M.D. Rosenblum. 2020. Regulatory T cells in skin injury: At the crossroads of tolerance and tissue repair. *Sci. Immunol.* 5:eaaz9631. https://doi.org/10.1126/sciimmunol.aaz9631

Boothby, I.C., M.J. Kinet, D.P. Boda, E.Y. Kwan, S. Clancy, J.N. Cohen, I. Habrylo, M.M. Lowe, M. Pauli, A.E. Yates, et al. 2021. Early-life inflammation primes a T helper 2 cell-fibroblast niche in skin. *Nature.* 599:667–672. https://doi.org/10.1038/s41586-021-04044-7

Break, T.J., V. Oikonomou, N. Dutzan, J.V. Desai, M. Swidergall, T. Freiwald, D. Chauss, O.J. Harrison, J. Alejo, D.W. Williams, et al. 2021. Aberrant type 1 immunity drives susceptibility to mucosal fungal infections. *Science.* 371:eaay5731. https://doi.org/10.1126/science.aay5731

Brown, A.F., J.M. Leech, T.R. Rogers, and R.M. McLoughlin. 2014. Staphylococcus aureus colonization: Modulation of host immune response and impact on human vaccine design. *Front. Immunol.* 4:507. https://doi.org/10.3389/fimmu.2013.00507

Brown, A.F., A.G. Murphy, S.J. Lalor, J.M. Leech, K.M. O'Keeffe, M. Mac Aogáin, D.P. O'Halloran, K.A. Lacey, M. Tavakol, C.H. Hearnden, et al. 2015. Memory Th1 cells are protective in invasive Staphylococcus aureus infection. *PLoS Pathog.* 11:e1005226. https://doi.org/10.1371/journal.ppat.1005226

Bunn, P.T., M. Montes de Oca, F. de Labastida Rivera, R. Kumar, S.S. Ng, C.L. Edwards, R.J. Faleiro, M. Sheel, F.H. Amante, T.C.M. Frame, et al. 2018. Distinct roles for CD4+ Foxp3+ regulatory T cells and IL-10-mediated immunoregulatory mechanisms during experimental visceral leishmaniasis caused by Leishmania donovani. *J. Immunol.* 201:3362–3372. https://doi.org/10.4049/jimmunol.1701582

Byrd, A.L., C. Deming, S.K.B. Cassidy, O.J. Harrison, W.I. Ng, S. Conlan, NISC Comparative Sequencing Program, Y. Belkaid, J.A. Segre, and H.H. Kong. 2017. Staphylococcus aureus and Staphylococcus epidermidis strain diversity underlying pediatric atopic dermatitis. *Sci. Transl. Med.* 9: eaal4651. https://doi.org/10.1126/scitranslmed.aal4651

Campanelli, A.P., A.M. Roselino, K.A. Cavassani, M.S.F. Pereira, R.A. Mortara, C.I. Brodskyn, H.S. Goncalves, Y. Belkaid, M. Barral-Netto, A. Barral, and J.S. Silva. 2006. CD4+CD25+ T cells in skin lesions of patients with cutaneous leishmaniasis exhibit phenotypic and functional characteristics of natural regulatory T cells. *J. Infect. Dis.* 193:1313–1322. https://doi.org/10.1086/502980

Chang, H.W., D. Yan, R. Singh, J. Liu, X. Lu, D. Ucmak, K. Lee, L. Afifi, D. Fadrosh, J. Leech, et al. 2018. Alteration of the cutaneous microbiome in psoriasis and potential role in Th17 polarization. *Microbiome.* 6:154. https://doi.org/10.1186/s40168-018-0533-1

Charmoy, M., B.P. Hurrell, A. Romano, S.H. Lee, F. Ribeiro-Gomes, N. Riteau, K. Mayer-Barber, F. Tacchini-Cottier, and D.L. Sacks. 2016. The Nlrp3 inflammasome, IL-1β, and neutrophil recruitment are required for susceptibility to a nonhealing strain of Leishmania major in C57BL/6 mice. *Eur. J. Immunol.* 46:897–911. https://doi.org/10.1002/eji.201546015

Cho, J.S., E.M. Pietras, N.C. Garcia, R.I. Ramos, D.M. Farzam, H.R. Monroe, J.E. Magorien, A. Blauvelt, J.K. Kolls, A.L. Cheung, et al. 2010. IL-17 is essential for host defense against cutaneous Staphylococcus aureus infection in mice. *J. Clin. Invest.* 120:1762–1773. https://doi.org/10.1172/JCI40891

Clegg, J., E. Soldaini, F. Bagnoli, and R.M. McLoughlin. 2021. Targeting skin-resident memory T cells via vaccination to combat Staphylococcus aureus infections. *Trends Immunol.* 42:6–17. https://doi.org/10.1016/j.it.2020.11.005

Costa, D.L., L.H. Guimarães, T.M. Cardoso, A. Queiroz, E. Lago, A.M. Roselino, O. Bacellar, E.M. Carvalho, and J.S. Silva. 2013. Characterization of regulatory T cell (Treg) function in patients infected with Leishmania braziliensis. *Hum. Immunol.* 74:1491–1500. https://doi.org/10.1016/j.humimm.2013.08.269

Cruz, A., S.A. Khader, E. Torrado, A. Fraga, J.E. Pearl, J. Pedrosa, A.M. Cooper, and A.G. Castro. 2006. Cutting edge: IFN-Gamma regulates the induction and expansion of IL-17-producing CD4 T cells during mycobacterial infection. *J. Immunol.* 177:1416–1420. https://doi.org/10.4049/jimmunol.177.3.1416

De Francesco, M.A., and A. Caruso. 2022. The gut microbiome in psoriasis and crohn's disease: Is its perturbation a common denominator for their pathogenesis? *Vaccines.* 10:244. https://doi.org/10.3390/vaccines10020244

Di Giovangiulio, M., A. Rizzo, E. Franzè, F. Caprioli, F. Facciotti, S. Onali, A. Favale, C. Stolfi, H.J. Fehling, G. Monteleone, and M.C. Fantini.

2019. Tbet expression in regulatory T cells is required to initiate Th1-mediated colitis. *Front. Immunol.* 10:2158. https://doi.org/10.3389/fimmu.2019.02158

Ehrlich, A., T.M. Castilho, K. Goldsmith-Pestana, W.J. Chae, A.L.M. Bothwell, T. Sparwasser, and D. McMahon-Pratt. 2014. The immunotherapeutic role of regulatory T cells in Leishmania (Viannia) panamensis infection. *J. Immunol.* 193:2961–2970. https://doi.org/10.4049/jimmunol.1400728

Falcão, S. C., T.R. de Moura, J. Clarencio, C.Brodskyn, A.Barral, and C.I.de Oliveira. 2012. The presence of Tregs does not preclude immunity to reinfection with Leishmania braziliensis. *Int. J. Parasitol.* 42:771–780. https://doi.org/10.1016/j.ijpara.2012.05.006

Flowers, L., and E.A. Grice. 2020. The skin microbiota: Balancing risk and reward. *Cell Host Microbe.* 28:190–200. https://doi.org/10.1016/j.chom.2020.06.017

Fyhrquist, N., G. Muirhead, S. Prast-Nielsen, M. Jeanmougin, P. Olah, T. Skoog, G. Jules-Clement, M. Feld, M. Barrientos-Somarribas, H. Sinkko, et al. 2019. Microbe-host interplay in atopic dermatitis and psoriasis. *Nat. Commun.* 10:4703. https://doi.org/10.1038/s41467-019-12253-y

Geoghegan, J.A., A.D. Irvine, and T.J. Foster. 2018. Staphylococcus aureus and atopic dermatitis: A complex and evolving relationship. *Trends Microbiol.* 26:484–497. https://doi.org/10.1016/j.tim.2017.11.008

Gimblet, C., J.S. Meisel, M.A. Loesche, S.D. Cole, J. Horwinski, F.O. Novais, A.M. Misic, C.W. Bradley, D.P. Beiting, S.C. Rankin, et al. 2017. Cutaneous leishmaniasis induces a transmissible dysbiotic skin microbiota that promotes skin inflammation. *Cell Host Microbe.* 22:13–24.e4. https://doi.org/10.1016/j.chom.2017.06.006

Gonçalves-de-Albuquerque, S.D.C., R. Pessoa-E-Silva, L.A.M. Trajano-Silva, T.C. de Goes, R.C.S. de Morais, C.N. da C Oliveira, V.M.B. de Lorena, and M. de Paiva-Cavalcanti. 2017. The equivocal role of Th17 cells and neutrophils on immunopathogenesis of leishmaniasis. *Front. Immunol.* 8:1437. https://doi.org/10.3389/fimmu.2017.01437

Gonzalez-Lombana, C., C. Gimblet, O. Bacellar, W.W. Oliveira, S. Passos, L.P. Carvalho, M. Goldschmidt, E.M. Carvalho, and P. Scott. 2013. IL-17 mediates immunopathology in the absence of IL-10 following Leishmania major infection. *PLoS Pathog.* 9:e1003243. https://doi.org/10.1371/journal.ppat.1003243

Gouirand, V., I. Habrylo, and M.D. Rosenblum. 2022. Regulatory T cells and inflammatory mediators in autoimmune disease. *J. Invest. Dermatol.* 142: 774–780. https://doi.org/10.1016/j.jid.2021.05.010

Grice, E.A., E.S. Snitkin, L.J. Yockey, D.M. Bermudez, NISC Comparative Sequencing Program, K.W. Liechty, and J.A. Segre. 2010. Longitudinal shift in diabetic wound microbiota correlates with prolonged skin defense response. *Proc. Natl. Acad. Sci. USA.* 107:14799–14804. https://doi.org/10.1073/pnas.1004204107

Harrington, L.E., R.D. Hatton, P.R. Mangan, H. Turner, T.L. Murphy, K.M. Murphy, and C.T. Weaver. 2005. Interleukin 17-producing CD4+ effector T cells develop via a lineage distinct from the T helper type 1 and 2 lineages. *Nat. Immunol.* 6:1123–1132. https://doi.org/10.1038/ni1254

Harrison, O.J., J.L. Linehan, H.Y. Shih, N. Bouladoux, S.J. Han, M. Smelkinson, S.K. Sen, A.L. Byrd, M. Enamorado, C. Yao, et al. 2019. Commensal-specific T cell plasticity promotes rapid tissue adaptation to injury. *Science.* 363:eaat6280. https://doi.org/10.1126/science.aat6280

Hartwig, T., P. Zwicky, B. Schreiner, N. Yawalkar, P. Cheng, A. Navarini, R. Dummer, L. Flatz, C. Conrad, C. Schlapbach, and B. Becher. 2018. Regulatory T cells restrain pathogenic T helper cells during skin inflammation. *Cell Rep.* 25:3564–3572 e4. https://doi.org/10.1016/j.celrep.2018.12.012

Hu, X., and L.B. Ivashkiv. 2009. Cross-regulation of signaling pathways by interferon-gamma: Implications for immune responses and autoimmune diseases. *Immunity.* 31:539–550. https://doi.org/10.1016/j.immuni.2009.09.002

Hu, W., Z.M. Wang, Y. Feng, M. Schizas, B.E. Hoyos, J. van der Veeken, J.G. Verter, R. Bou-Puerto, and A.Y. Rudensky. 2021. Regulatory T cells function in established systemic inflammation and reverse fatal autoimmunity. *Nat. Immunol.* 22:1163–1174. https://doi.org/10.1038/s41590-021-01001-4

Kalekar, L.A., J.N. Cohen, N. Prevel, P.M. Sandoval, A.N. Mathur, J.M. Moreau, M.M. Lowe, A. Nosbaum, P.J. Wolters, A. Haemel, et al. 2019. Regulatory T cells in skin are uniquely poised to suppress profibrotic immune responses. *Sci. immunol.* 4:eaaw2910. https://doi.org/10.1126/sciimmunol.aaw2910

Kaye, P., and P. Scott. 2011. Leishmaniasis: Complexity at the host-pathogen interface. *Nat. Rev. Microbiol.* 9:604–615. https://doi.org/10.1038/nrmicro2608

Kim, J.M., J.P. Rasmussen, and A.Y. Rudensky. 2007. Regulatory T cells prevent catastrophic autoimmunity throughout the lifespan of mice. *Nat. Immunol.* 8:191–197. https://doi.org/10.1038/ni1428

Kobayashi, T., M. Glatz, K. Horiuchi, H. Kawasaki, H. Akiyama, D.H. Kaplan, H.H. Kong, M. Amagai, and K. Nagao. 2015. Dysbiosis and Staphylococcus aureus colonization drives inflammation in atopic dermatitis. *Immunity*. 42:756–766. https://doi.org/10.1016/j.immuni.2015.03.014

Koch, M.A., G. Tucker-Heard, N.R. Perdue, J.R. Killebrew, K.B. Urdahl, and D.J. Campbell. 2009. The transcription factor T-bet controls regulatory T cell homeostasis and function during type 1 inflammation. *Nat. Immunol*. 10:595–602. https://doi.org/10.1038/ni.1731

Leech, J.M., M.O. Dhariwala, M.M. Lowe, K. Chu, G.R. Merana, C. Cornuot, A. Weckel, J.M. Ma, E.G. Leitner, J.R. Gonzalez, et al. 2019. Toxin-triggered interleukin-1 receptor signaling enables early-life discrimination of pathogenic versus commensal skin bacteria. *Cell Host Microbe*. 26: 795–809.e5. https://doi.org/10.1016/j.chom.2019.10.007

Liang, X., C. Ou, J. Zhuang, J. Li, F. Zhang, Y. Zhong, and Y. Chen. 2021. Interplay between skin microbiota dysbiosis and the host immune system in psoriasis: Potential pathogenesis. *Front. Immunol*. 12:764384. https://doi.org/10.3389/fimmu.2021.764384

Liu, H., N.K. Archer, C.A. Dillen, Y. Wang, A.G. Ashbaugh, R.V. Ortines, T. Kao, S.K. Lee, S.S. Cai, R.J. Miller, et al. 2017. Staphylococcus aureus epicutaneous exposure drives skin inflammation via IL-36-mediated T cell responses. *Cell Host Microbe*. 22:653–666.e5. https://doi.org/10.1016/j.chom.2017.10.006

Liu, Y., H. Wang, M. Taylor, C. Cook, A. Martínez-Berdeja, J.P. North, P. Harirchian, A.A. Hailer, Z. Zhao, R. Ghadially, et al. 2022. Classification of human chronic inflammatory skin disease based on single-cell immune profiling. *Sci. Immunol*. 7:eabl9165. https://doi.org/10.1126/sciimmunol.abl9165

Lopez Kostka, S., S. Dinges, K. Griewank, Y. Iwakura, M.C. Udey, and E. von Stebut. 2009. IL-17 promotes progression of cutaneous leishmaniasis in susceptible mice. *J. Immunol*. 182:3039–3046. https://doi.org/10.4049/jimmunol.0713598

Malhotra, N., J.M. Leyva-Castillo, U. Jadhav, O. Barreiro, C. Kam, N.K. O'Neill, F. Meylan, P. Chambon, U.H. von Andrian, R.M. Siegel, et al. 2018. RORα-expressing T regulatory cells restrain allergic skin inflammation. *Sci. Immunol*. 3:eaao6923. https://doi.org/10.1126/sciimmunol.aao6923

Mathur, A.N., B. Zirak, I.C. Boothby, M. Tan, J.N. Cohen, T.M. Mauro, P. Mehta, M.M. Lowe, A.K. Abbas, N. Ali, and M.D. Rosenblum. 2019. Treg-cell control of a CXCL5-IL-17 inflammatory Axis promotes hair-follicle-stem-cell differentiation during skin-barrier repair. *Immunity*. 50:655–667.e4. https://doi.org/10.1016/j.immuni.2019.02.013

Mendez, S., S.K. Reckling, C.A. Piccirillo, D. Sacks, and Y. Belkaid. 2004. Role for CD4(+) CD25(+) regulatory T cells in reactivation of persistent leishmaniasis and control of concomitant immunity. *J. Exp. Med*. 200: 201–210. https://doi.org/10.1084/jem.20040298

Miller, L.S., and J.S. Cho. 2011. Immunity against Staphylococcus aureus cutaneous infections. *Nat. Rev. Immunol*. 11:505–518. https://doi.org/10.1038/nri3010

Montgomery, C.P., M. Daniels, F. Zhao, M.L. Alegre, A.S. Chong, and R.S. Daum. 2014. Protective immunity against recurrent Staphylococcus aureus skin infection requires antibody and interleukin-17A. *Infect. Immun*. 82:2125–2134. https://doi.org/10.1128/IAI.01491-14

Moreau, J.M., M.O. Dhariwala, V. Gouirand, D.P. Boda, I.C. Boothby, M.M. Lowe, J.N. Cohen, C.E. Macon, J.M. Leech, L.A. Kalekar, et al. 2021. Regulatory T cells promote innate inflammation after skin barrier breach via TGF-β activation. *Sci. Immunol*. 6:eabg2329. https://doi.org/10.1126/sciimmunol.abg2329

Naik, S., N. Bouladoux, C. Wilhelm, M.J. Molloy, R. Salcedo, W. Kastenmuller, C. Deming, M. Quinones, L. Koo, S. Conlan, et al. 2012. Compartmentalized control of skin immunity by resident commensals. *Science*. 337: 1115–1119. https://doi.org/10.1126/science.1225152

Nakagawa, S., M. Matsumoto, Y. Katayama, R. Oguma, S. Wakabayashi, T. Nygaard, S. Saijo, N. Inohara, M. Otto, H. Matsue, et al. 2017. Staphylococcus aureus virulent PSMα peptides induce keratinocyte alarmin release to orchestrate IL-17-dependent skin inflammation. *Cell Host Microbe*. 22:667–677.e5. https://doi.org/10.1016/j.chom.2017.10.008

Nosbaum, A., N. Prevel, H.A. Truong, P. Mehta, M. Ettinger, T.C. Scharschmidt, N.H. Ali, M.L. Pauli, A.K. Abbas, and M.D. Rosenblum. 2016. Cutting edge: Regulatory T cells facilitate cutaneous wound healing. *J. Immunol*. 196:2010–2014. https://doi.org/10.4049/jimmunol.1502139

Novais, F.O., A.M. Carvalho, M.L. Clark, L.P. Carvalho, D.P. Beiting, I.E. Brodsky, E.M. Carvalho, and P. Scott. 2017. CD8+ T cell cytotoxicity mediates pathology in the skin by inflammasome activation and IL-1β production. *PLoS Pathog*. 13:e1006196. https://doi.org/10.1371/journal.ppat.1006196

Pandiyan, P., N. Bhaskaran, M. Zou, E. Schneider, S. Jayaraman, and J. Huehn. 2019. Microbiome dependent regulation of T_{regs} and Th17 cells in mucosa. *Front. Immunol*. 10:426. https://doi.org/10.3389/fimmu.2019.00426

Pedraza-Zamora, C.P., J. Delgado-Dominguez, J. Zamora-Chimal, and I. Becker. 2017. Th17 cells and neutrophils: Close collaborators in chronic Leishmania mexicana infections leading to disease severity. *Parasite Immunol*. 39. https://doi.org/10.1111/pim.12420

Rebane, A., M. Zimmermann, A. Aab, H. Baurecht, A. Koreck, M. Karelson, K. Abram, T. Metsalu, M. Pihlap, N. Meyer, et al. 2012. Mechanisms of IFN-gamma-induced apoptosis of human skin keratinocytes in patients with atopic dermatitis. *J. Allergy Clin. Immunol*. 129:1297–1306. https://doi.org/10.1016/j.jaci.2012.02.020

Rodriguez-Pinto, D., A. Navas, V.M. Blanco, L. Ramírez, D. Garcerant, A. Cruz, N. Craft, and N.G. Saravia. 2012. Regulatory T cells in the pathogenesis and healing of chronic human dermal leishmaniasis caused by Leishmania (Viannia) species. *PLoS Negl. Trop. Dis*. 6:e1627. https://doi.org/10.1371/journal.pntd.0001627

Salgado, V.R., A.T.L. de Queiroz, S.S. Sanabani, C.I. de Oliveira, E.M. Carvalho, J.M.L. Costa, M. Barral-Netto, and A. Barral. 2016. The microbiological signature of human cutaneous leishmaniasis lesions exhibits restricted bacterial diversity compared to healthy skin. *Mem. Inst. Oswaldo Cruz*. 111:241–251. https://doi.org/10.1590/0074-02760150436

Santos, D., T.M. Campos, M. Saldanha, S.C. Oliveira, M. Nascimento, D.S. Zamboni, P.R. Machado, S. Arruda, P. Scott, E.M. Carvalho, and L.P. Carvalho. 2018. IL-1β production by intermediate monocytes is associated with immunopathology in cutaneous leishmaniasis. *J. Invest. Dermatol*. 138:1107–1115. https://doi.org/10.1016/j.jid.2017.11.029

Scharschmidt, T.C., K.S. Vasquez, H.A. Truong, S.V. Gearty, M.L. Pauli, A. Nosbaum, I.K. Gratz, M. Otto, J.J. Moon, J. Liese, et al. 2015. A wave of regulatory T cells into neonatal skin mediates tolerance to commensal microbes. *Immunity*. 43:1011–1021. https://doi.org/10.1016/j.immuni.2015.10.016

Scott, P., and F.O. Novais. 2016. Cutaneous leishmaniasis: Immune responses in protection and pathogenesis. *Nat. Rev. Immunol*. 16:581–592. https://doi.org/10.1038/nri.2016.72

Sefik, E., N. Geva-Zatorsky, S. Oh, L. Konnikova, D. Zemmour, A.M. McGuire, D. Burzyn, A. Ortiz-Lopez, M. Lobera, J. Yang, et al. 2015. MUCOSAL IMMUNOLOGY. Individual intestinal symbionts induce a distinct population of RORγ+ regulatory T cells. *Science*. 349:993–997. https://doi.org/10.1126/science.aaa9420

Shao, S., L.C. Tsoi, M.K. Sarkar, X. Xing, K. Xue, R. Uppala, C.C. Berthier, C. Zeng, M. Patrick, A.C. Billi, et al. 2019. IFN-γ enhances cell-mediated cytotoxicity against keratinocytes via JAK2/STAT1 in lichen planus. *Sci. Transl. Med*. 11:eaav7561. https://doi.org/10.1126/scitranslmed.aav7561

Singh, T.P., A.M. Carvalho, L.A. Sacramento, E.A. Grice, and P. Scott. 2021. Microbiota instruct IL-17A-producing innate lymphoid cells to promote skin inflammation in cutaneous leishmaniasis. *PLoS Pathog*. 17:e1009693. https://doi.org/10.1371/journal.ppat.1009693

Späth, G.F., and S.M. Beverley. 2001. A lipophosphoglycan-independent method for isolation of infective Leishmania metacyclic promastigotes by density gradient centrifugation. *Exp. Parasitol*. 99:97–103. https://doi.org/10.1006/expr.2001.4656

Stumhofer, J.S., A. Laurence, E.H. Wilson, E. Huang, C.M. Tato, L.M. Johnson, A.V. Villarino, Q. Huang, A. Yoshimura, D. Sehy, et al. 2006. Interleukin 27 negatively regulates the development of interleukin 17-producing T helper cells during chronic inflammation of the central nervous system. *Nat. Immunol*. 7:937–945. https://doi.org/10.1038/ni1376

Terui, H., K. Yamasaki, M. Wada-Irimada, N. Onodera-Amagai, N. Hatchome, M. Mizuashi, R. Yamashita, T. Kawabe, N. Ishii, T. Abe, et al. 2022. Staphylococcus aureus Skin colonization promotes SLE-like autoimmune inflammation via neutrophil activation and the IL-23/IL-17 axis. *Sci. Immunol*. 7:eabm9811. https://doi.org/10.1126/sciimmunol.abm9811

Trautmann, A., M. Akdis, P. Schmid-Grendelmeier, R. Disch, E.B. Bröcker, K. Blaser, and C.A. Akdis. 2001. Targeting keratinocyte apoptosis in the treatment of atopic dermatitis and allergic contact dermatitis. *J. Allergy Clin. Immunol*. 108:839–846. https://doi.org/10.1067/mai.2001.118796

Tuffs, S.W., M.I. Goncheva, S.X. Xu, H.C. Craig, K.J. Kasper, J. Choi, R.S. Flannagan, S.M. Kerfoot, D.E. Heinrichs, and J.K. McCormick. 2022. Superantigens promote Staphylococcus aureus bloodstream infection by eliciting pathogenic interferon-gamma production. *Proc. Natl. Acad. Sci. USA*. 119:e2115987119. https://doi.org/10.1073/pnas.2115987119

Unger, A., S. O'Neal, P.R. Machado, L.H. Guimarães, D.J. Morgan, A. Schriefer, O. Bacellar, M.J. Glesby, and E.M. Carvalho. 2009. Association of treatment of American cutaneous leishmaniasis prior to ulcer development

with high rate of failure in northeastern Brazil. *Am. J. Trop. Med. Hyg.* 80: 574–579. https://doi.org/10.4269/ajtmh.2009.80.574

van der Fits, L., S. Mourits, J.S.A. Voerman, M. Kant, L. Boon, J.D. Laman, F. Cornelissen, A.M. Mus, E. Florencia, E.P. Prens, and E. Lubberts. 2009. Imiquimod-induced psoriasis-like skin inflammation in mice is mediated via the IL-23/IL-17 axis. *J. Immunol.* 182:5836–5845. https://doi.org/10.4049/jimmunol.0802999

Viard-Leveugle, I., O. Gaide, D. Jankovic, L. Feldmeyer, K. Kerl, C. Pickard, S. Roques, P.S. Friedmann, E. Contassot, and L.E. French. 2013. TNF-α and IFN-γ are potential inducers of Fas-mediated keratinocyte apoptosis through activation of inducible nitric oxide synthase in toxic epidermal necrolysis. *J. Invest. Dermatol.* 133:489–498. https://doi.org/10.1038/jid.2012.330

Whibley, N., A. Tucci, and F. Powrie. 2019. Regulatory T cell adaptation in the intestine and skin. *Nat. Immunol.* 20:386–396. https://doi.org/10.1038/s41590-019-0351-z

Wohlfert, E.A., J.R. Grainger, N. Bouladoux, J.E. Konkel, G. Oldenhove, C.H. Ribeiro, J.A. Hall, R. Yagi, S. Naik, R. Bhairavabhotla, et al. 2011. GATA3 controls Foxp3⁺ regulatory T cell fate during inflammation in mice. *J. Clin. Invest.* 121:4503–4515. https://doi.org/10.1172/JCI57456
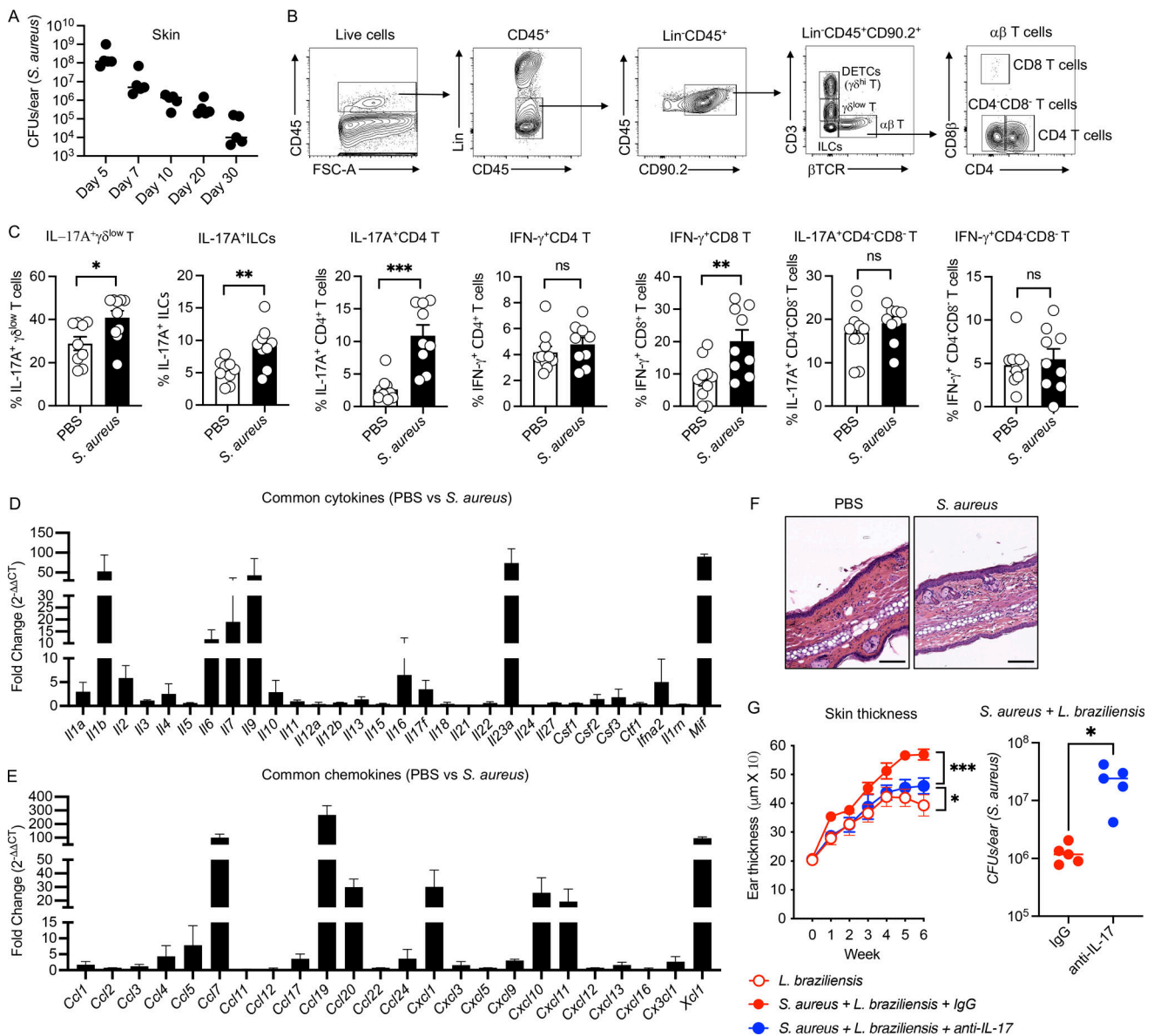
Supplemental material

Figure S1. **Topical colonization of *S. aureus* induces dominant type-17 signature. (A)** Enumeration of CFUs of *S. aureus* at day 5, 7, 10, 20, and 30 from the ears of *S. aureus*–colonized mice. Representative of one experiment with five mice in each group. **(B)** Gating strategy to identify the T cells and ILCs in ear skin by flow cytometry. Representative of more than two experiments with 9–10 mice per group. **(C)** Percent of IL-17A and IFN-γ from γδ^{low} T, CD4 T, CD8 T, and CD4$^-$CD8$^-$ T cells and ILCs in the skin of PBS and *S. aureus*–colonized mice at day 10 by flow cytometry. Mean ± SEM from two experiments with 9–10 per mice group. **(D and E)** Analysis of mRNA transcript of cytokines and chemokines in *S. aureus*–colonized mice at day 10. Data represented as FC over PBS control and pooled from two experiments. RNA pooled from three mice in each experiment. Mean ± SEM from two experiments with six mice per mice group. **(F)** H&E-stained sections of ear skin from PBS control or *S. aureus*–colonized mice at day 10 (scale bar = 200 mm). **(G)** Skin thickness and *S. aureus* CFUs in IgG and anti–IL-17 injected mice as indicated. Mean ± SD representative of one experiment with five mice in each group. *P < 0.05, **P < 0.01, and ***P < 0.001. "ns" denotes not significant. Significant P values by two-tailed unpaired Student's *t* test with Welch's correction are indicated in the figure.
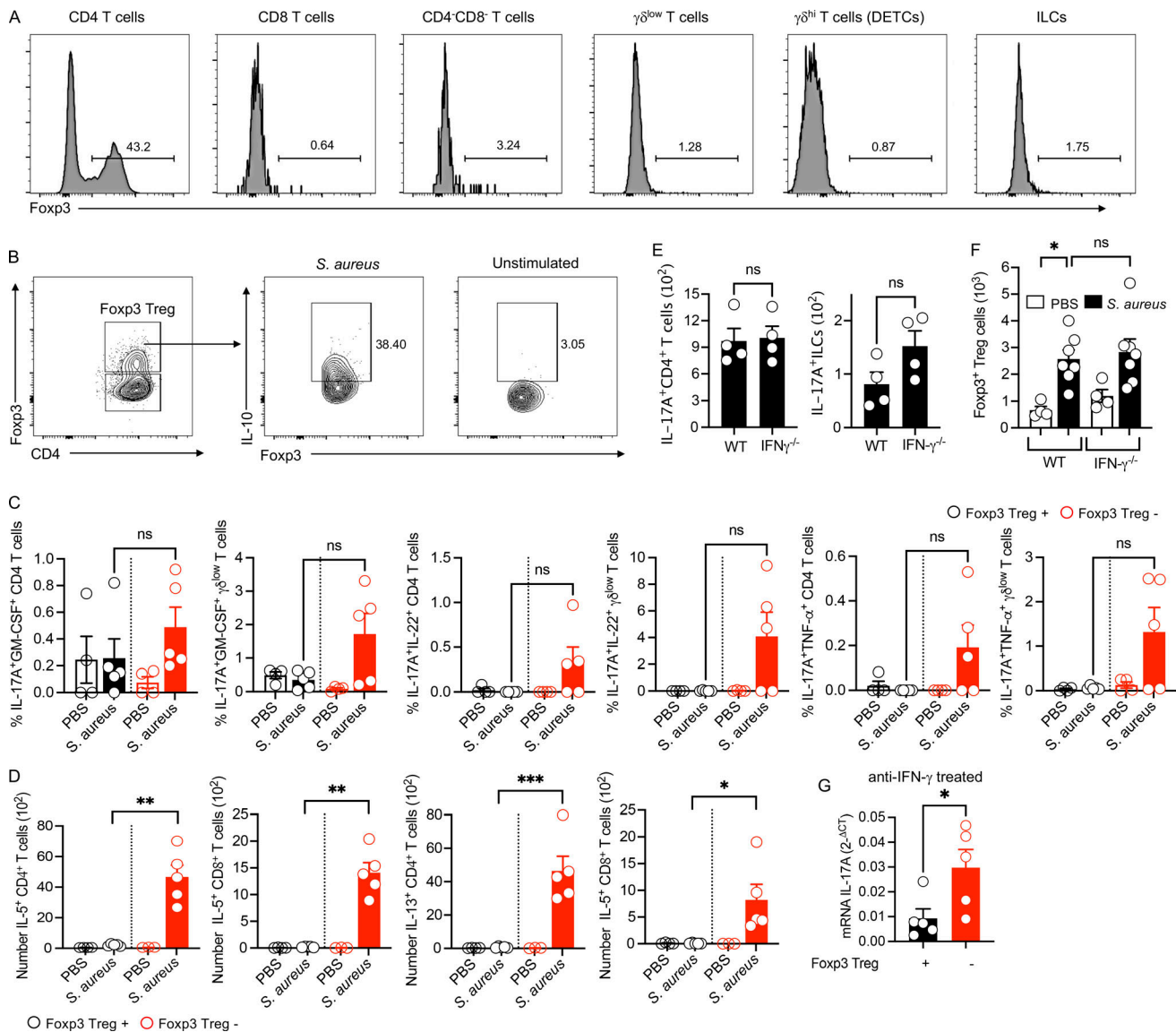
Figure S2. **Characterization of skin Foxp3⁺Treg cells and impact of Foxp3⁺ Treg cell depletion after topical *S. aureus* colonization. (A)** Representative flow cytometric analysis of Foxp3 expression on CD4 T, CD8 T, CD4⁻CD8⁻ T, γδ^low T, γδ^hi T cells, and ILCs after *S. aureus* colonization on day 10. Representative of two experiments with four mice per group. Numbers in contour plots indicate the percent of cells within the gates. **(B)** Representative flow cytometric analysis of IL-10 in Foxp3⁺ Treg cells in *S. aureus*–colonized mice on day 10. Representative of one experiment with five mice per group. Numbers in contour plots indicate the percent of cells within the gates. **(C)** Percent of IL-17⁺GM-CSF⁺, IL-17⁺IL-22⁺, IL-17⁺TNF-α⁺, and/or IL-17⁺IL-10⁺ from CD4 T and γδ^low T and in Foxp3⁺ Treg-depleted and non-depleted Foxp3-DTR mice after *S. aureus* colonization on day 10. Mean ± SEM representative of one experiment with four to five mice per group. **(D)** Number of IL-5 and IL-13–producing CD4 and CD8 T cells in Foxp3⁺ Treg-depleted and non-depleted Foxp3-DTR mice after *S. aureus* colonization on day 10. Mean ± SEM representative of two experiments with four to five mice per group. **(E)** Number of IL-17–producing CD4 T cells and ILCs in WT and IFN-γ⁻/⁻ on day 10 after *S. aureus* colonization. Mean ± SEM representative of two experiments with four mice per group. **(F)** Foxp3⁺ Treg cells in wild-type and IFN-γ⁻/⁻ mice after *S. aureus* colonization. **(G)** qRT-PCR analysis of *Il17a* in Foxp3⁺ Treg-depleted Foxp3-DTR and non-depleted wild-type mice after *S. aureus* colonization at day 10, injected with anti–IFN-γ. Mean ± SEM from two experiments with four to seven mice per group. *P < 0.05, **P < 0.01, and ***P < 0.001. "ns" denotes not significant. Significant P values by two-tailed unpaired Student's *t* test with Welch's correction are indicated in the figure.
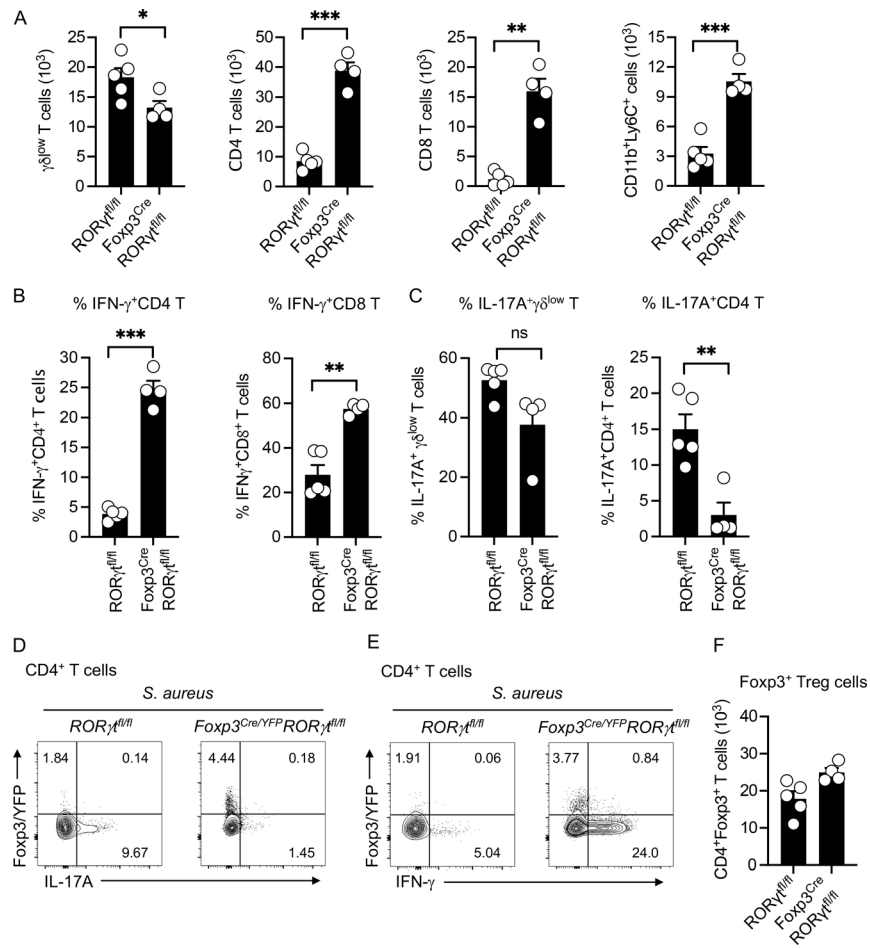
Figure S3. **RORγt⁺ Foxp3⁺ Treg cells control the IFN-γ–producing CD4 and CD8 T cells. (A)** Absolute cell numbers of γδ^{low} T, CD4 T, and CD8 T cells and monocytes in the skin of *S. aureus*–colonized *RORγt$^{fl/fl}$* and *Foxp3^{Cre}RORγt$^{fl/fl}$* mice on day 10. Mean ± SEM representative of two experiments with four to five mice per group. **(B)** Percent of IFN-γ⁺CD4 T and IFN-γ⁺CD8 T cells in the skin of *S. aureus*–colonized *RORγt$^{fl/fl}$* and *Foxp3^{Cre}RORγt$^{fl/fl}$* mice at day 10 by flow cytometry. Mean ± SEM representative of two experiments with four to five mice per group. **(C)** Percent of IL-17A⁺γδ^{low} T and IL-17A⁺CD4 T cells in the skin of *S. aureus*–colonized *RORγt$^{fl/fl}$* and *Foxp3-^{Cre}RORγt$^{fl/fl}$* mice at day 10 by flow cytometry. Mean ± SEM representative of two experiments with four to five mice per group. **(D and E)** Flow cytometry analysis of Foxp3^{YFP} and IL-17A and IFN-γ in CD4⁺ T cells in *S. aureus*–colonized *RORγt$^{fl/fl}$* and *Foxp3$^{Cre/YFP}$RORγt$^{fl/fl}$* mice at day 10. Representative of two experiments with four mice per group. Numbers in contour plots indicate the percent of cells within the gates. **(F)** Absolute cell numbers of Foxp3⁺ Treg cells in *S. aureus*–colonized *RORγt$^{fl/fl}$* and *Foxp3^{Cre}RORγt$^{fl/fl}$* mice at day 10. Mean ± SEM representative of one experiment with four to five mice per group. *P < 0.05, **P < 0.01, and ***P < 0.001. "ns" denotes not significant. Significant P values by two-tailed unpaired Student's *t* test with Welch's correction are indicated in the figure.
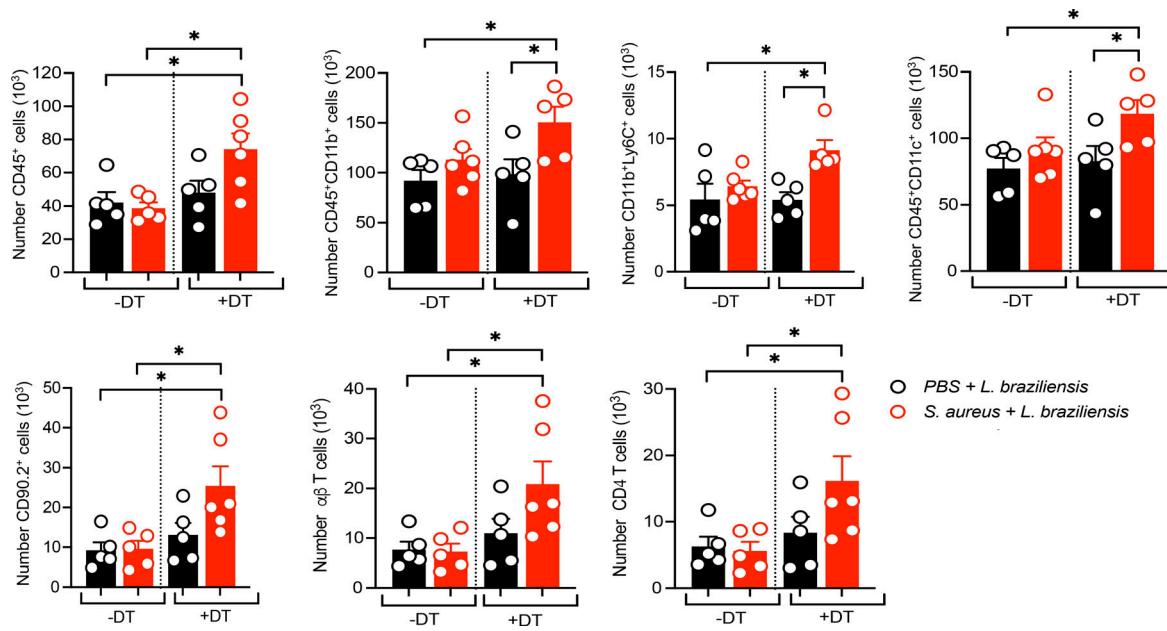
Figure S4. Impact of reduced Foxp3+ Tregs in _S. aureus_–colonized and _L. braziliensis_–infected mice. Foxp3-DTR heterozygous female mice were colonized on day 1–, and then at day 10 (week 0) mice were infected with _L. braziliensis_ in one ear as in Fig.2A and euthanized at week 6 for analysis. Mice treated with DT at weeks 0, 1, 2, 3, 4, and 5 to chronically reduce the Foxp3+ Tregs. Absolute numbers of CD45+, CD45+CD11b+, CD11b+Ly6C+, CD45+CD11c+, CD90.2+, αβ T cells, and CD4 T cells in the ear skin of different treatment groups of treated (+DT) and untreated (−DT) with DT at week 6. Mean ± SEM representative of one experiment with five to six mice per group. *P < 0.05. Significant P values by two-tailed unpaired Student's _t_ test with Welch's correction are indicated in the figure.
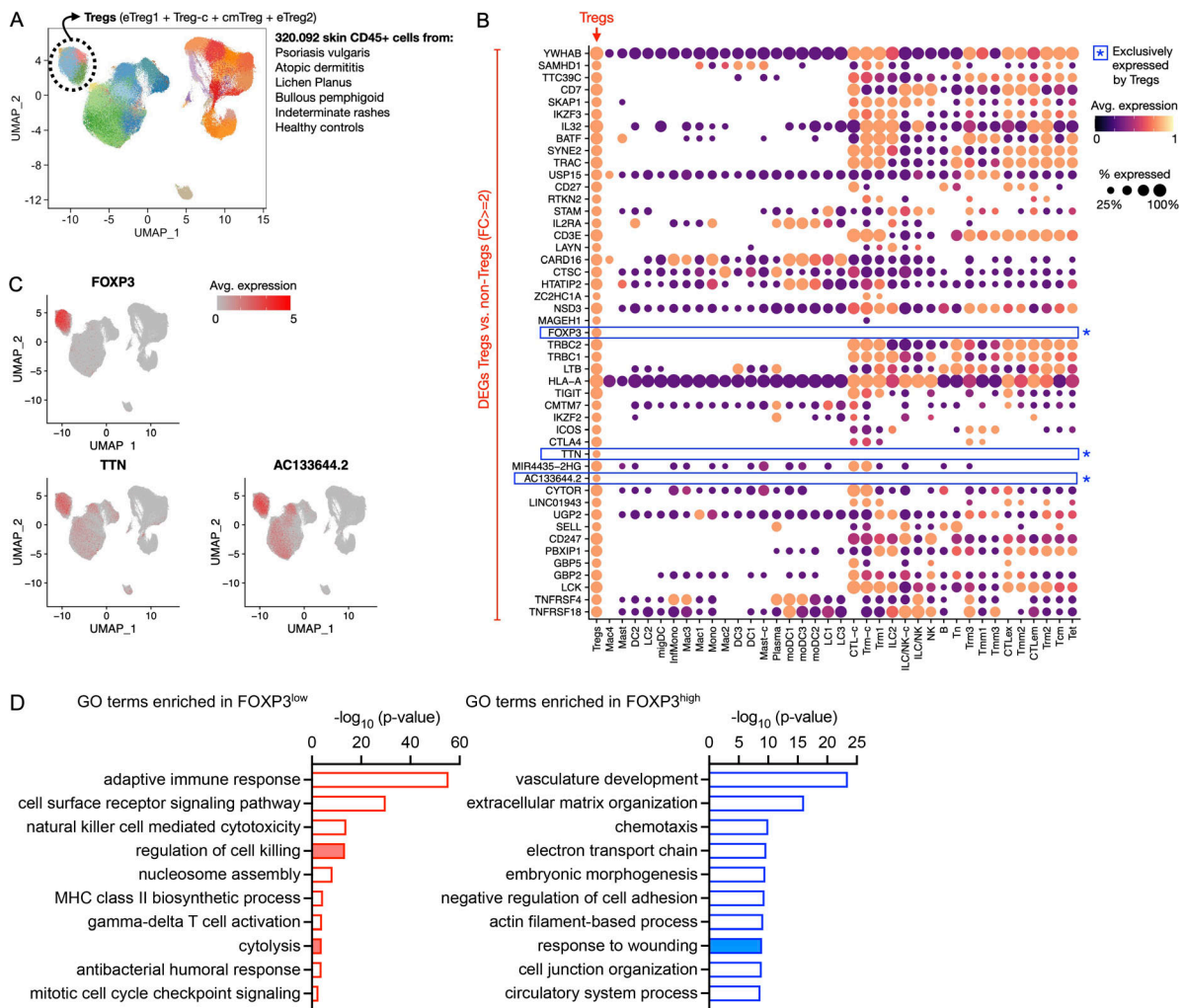
Figure S5. **Identification of *FOXP3* as a unique marker for human Tregs and analysis of *FOXP3*^{hi} and *FOXP3*^{low} enriched genes. (A)** Treg clusters are combined to one Treg population and visualized for *FOXP3* expression in all cell types. Data extracted from Liu et al. (2022). **(B)** Visualization of differently expressed genes in Treg cluster versus non-Treg cluster in different cell types. **(C)** *FOXP3*, *TTN*, and AC133644.2 expression in Treg and non-Treg clusters. **(D)** GO terms enrichment pathway analysis of genes associated with *FOXP3*^{high} and *FOXP3*^{low} by using Metascape Pathway analysis tool. Data were analyzed using differentially expressed genes from 19 *FOXP3*^{high}- and 20 *FOXP3*^{low}-expressing biopsies.

Provided online are four tables. Table S1 provides differential gene expression between FOXP3^{high} versus FOXP3^{low} samples. Table S2 provides a gene list for GO analysis using Metascape associated with FOXP3^{high} versus FOXP3^{low}. Table S3 provides Metascape results for Foxp3^{high} gene list. Table S4 provides Metascape results for Foxp3^{low} gene list.